Design and Operation of Hybrid Aeroacoustic Wind Tunnels

William Devenport
Center for Renewable Energy and Aerodynamic
Technology (CREATe)
Kevin T. Crofton Department of Aerospace and
Ocean Engineering
Virginia Tech, Blacksburg, Virginia 24060
UNITED STATES
devenport@vt.edu

Christian Bak
Department of Wind Energy
Technical University of Denmark
Risø Campus
Frederiksborgvej 399
4000 Roskilde
DENMARK
chba@dtu.dk

Kenneth Brown and **Aurélien Borgoltz**
CREATe, Kevin T. Crofton Department of
Aerospace and Ocean Engineering
Virginia Tech, Blacksburg, Virginia 24060
UNITED STATES

Jens Österlund
Fluid Thinking
Karlslundsvägen 18
12552 Stockholm
SWEDEN

Peter Davidsson
CREO Dynamics
Scheelvägen 27
223 63 Lund
SWEDEN

ABSTRACT

The concept of the hybrid anechoic wind tunnel is explained. Two such wind tunnels, the Virginia Tech Stability Wind Tunnel and the Poul la Cour Tunnel, currently under construction, are described in detail. These represent, respectively, hybrid anechoic facilities developed by retrofitting an existing aerodynamic wind tunnel, and designed from scratch. Some operational details of this type of wind tunnel are explained. Design considerations for both new and retrofitted facilities are described, from overall test section configuration to material properties of Kevlar cloth used to form acoustic windows. Finally, examples of an airfoil experiment are shown.

1.0   INTRODUCTION

Wind tunnels with a rectangular test section enclosed by hard walls (Figure 1-1) are ubiquitous for aerodynamic measurements and testing. These have become the standard for multiple reasons, but perhaps the most important is that interference corrections are small and well understood. Small corrections allow for successful testing of models that are large compared to the test section width up to, say, a chord to width ratio c/h of a half. The use of large models allows for testing at Reynolds numbers that more realistically represent practical applications. It also means that instrumentation mounted on or directed through the walls of the test section does not need to project over large distances to probe the flow around the model.

Sound measurements can be, and are, made in such test sections but this is only feasible for comparatively loud sources in large test sections. Outside of these cases, the requirement for high signal-to-noise ratio acoustic measurements dramatically changes the calculus of wind tunnel design. Hard walls serve as acoustic mirrors and thus confuse efforts to determine the location, directivity and strength of sound sources. Hard walls create a reverberant environment for parasitic noise sources associated with the wind tunnel circuit and fan, greatly increasing background noise levels. Microphones perform much better when placed outside the flow where they are not subjected to self-generated turbulent pressure fluctuations.

The conventional solution to these problems is the open jet configuration, where the wind tunnel walls are removed and the flow is launched across a large anechoic chamber in which acoustic instrumentation is placed. This can be a very effective design, but it is a design where aerodynamic performance takes second place to
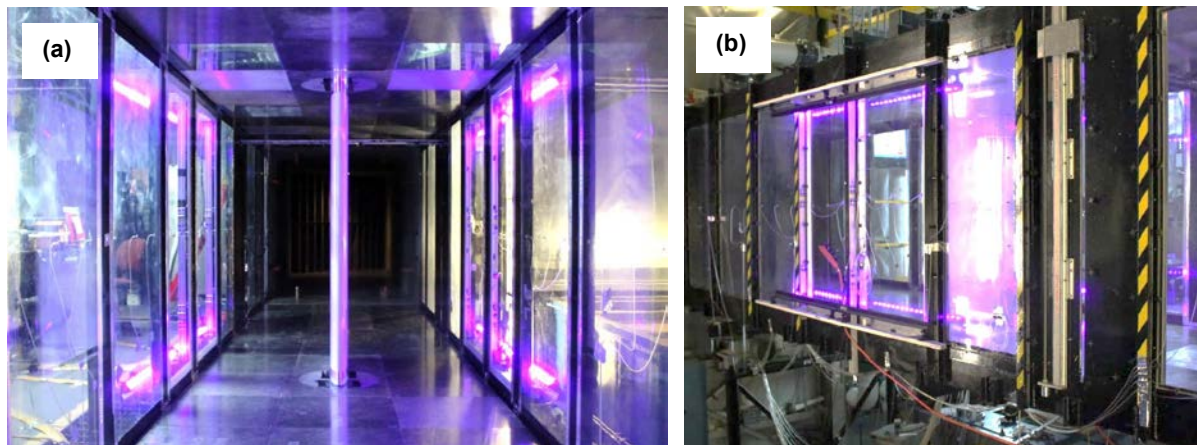
Figure 1-1: Hard-wall test section of the Virginia Tech Stability Tunnel with transparent wall panels installed. (a) View from inside the test section looking downstream with an airfoil model installed. (b) View from outside the port-side of the test section, looking upstream.

acoustic considerations. In some situations this can create undesirable effects. Interference corrections for lifting models in open-jet tunnels are large and angle of attack corrections of 50% of the geometric value (e.g. Brooks *et al.* [1]) are not uncommon and maybe a function of the model placement and shape details [2]. Indeed a lifting model will deflect the jet and unless the model is small compared to the test section, the relationship between the wind tunnel flow and free flight is compromised [3]. Making the model sufficiently small greatly reduces the Reynolds number range available for testing. A second problem is that the free jet shear layer grows rapidly with distance downstream. This limits the usable test section length, restricts the placement of microphones and other instrumentation, and can lead to parasitic noise generated by the interaction of shear layer turbulence with the test article. Turbulence in the jet and jet deflection make also the jet difficult to catch and re-absorb into the wind tunnel circuit in closed-circuit configurations, without generating parasitic noise and pulsations, and can complicate corrections for acoustic diffraction. The design of the collector can be particularly critical [4]. Buffeting by the jet turbulence limits the placement of microphone instrumentation close to the flow.

The basic concept of a hybrid aeroacoustic wind tunnel (Figure 1-2) is to combine the aerodynamic benefits of a closed arrangement with the acoustic benefits of an open arrangement. The test section is enclosed by walls resulting in small aerodynamic corrections, but the walls are at least partly acoustically transparent allowing sound measurements in a surrounding anechoic chamber. The hybrid tunnel was conceived of as a compromise – a way of converting an existing aerodynamic wind tunnel into a facility suitable for noise measurements when space and configuration limitations excluded the possibility of a free jet. However, the configuration results in a number of advantages compared to an open jet, including that: aerodynamic interference effects are reduced to hard-wall tunnel levels allowing for a higher Reynolds number range; a collector is not needed eliminating this source of unsteadiness and noise; microphones can be placed close to the exterior of the acoustic windows and thus near the test article where acoustic signal to noise ratio (SNR) is greater; the test section can be much longer than the equivalent free jet (a) allowing for greater spatial separation of the test article sound field from facility parasitic sources and thus further increase in SNR when beamforming using a phased array, and (b) allowing for a much greater range of streamwise directivity angles than might otherwise be possible. This is not to say, of course, that development and operation of such a facility is not without complications and challenges.
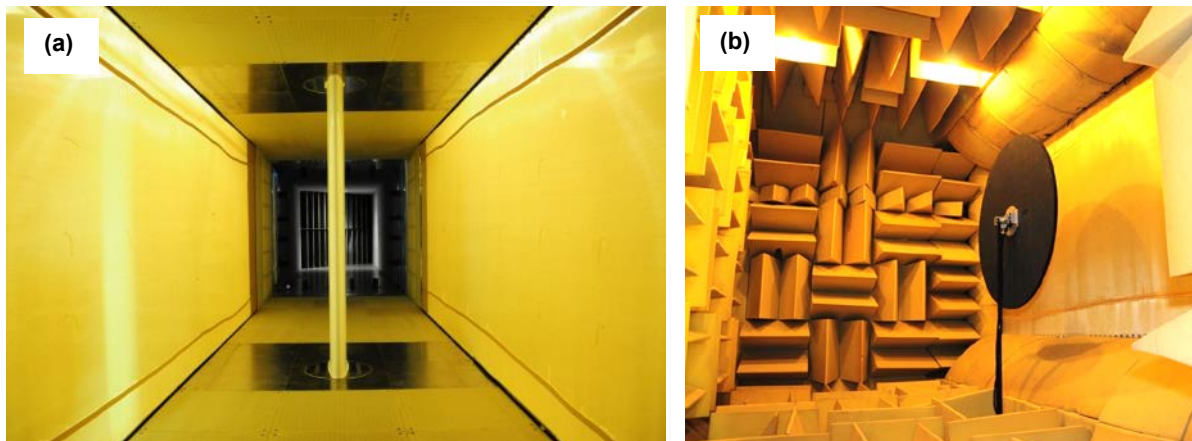
Figure 1-2: Hybrid anechoic test section of the Virginia Tech Stability Tunnel. (a) View from inside the test section looking downstream with an airfoil model installed. (b) View from outside the test section inside the port-side anechoic chamber looking upstream with a phased microphone array installed.

In this paper we attempt to document some of the practical choices and constraints that underpin the design and development of a successful hybrid anechoic tunnel. We also describe some of the details involved in effective operation of such a facility. We illustrate our discussion primarily with reference to two facilities; the Virginia Tech Stability Wind Tunnel, the original hybrid anechoic tunnel developed by conversion of an existing aerodynamic facility and; the Poul la Cour Tunnel, a facility currently under construction at the Technical University of Denmark (DTU) where this configuration has been incorporated from the start. We begin with a short overview of these facilities, and then discuss the principal operation and design elements.

2.0 TWO HYBRID ANECHOIC WIND TUNNELS

2.1 The Virginia Tech Stability Tunnel

The Virginia Tech Stability Tunnel was designed and built at NASA (then NACA) Langley in the late 1930s. It had interchangeable curved-flow and rolling-flow test sections intended for the measurement of aircraft stability derivatives. In the late 1950s the facility was dismantled and shipped to Virginia Tech where it was used for instruction and research. After prototype testing in 2004 and 2005 [5] a (then) novel hybrid anechoic test section system was designed and developed [6], including upgrades to the rest of the circuit to improve suitability for acoustic measurements. Along with other developments, this left the facility with two interchangeable test sections of the same internal dimensions – the hybrid anechoic section, and a conventional hard-wall test section. Over the last 10 years, the facility has been heavily used for education, fundamental research and industrial testing (particularly of wind turbine blade aerodynamics and aeroacoustics). Many refinements and improvements have been made in the course of this work, with much of what has been learned reflected in this document.

The tunnel forms a closed circuit, but has an air exchange tower open to the atmosphere to allow for temperature stabilization (Figure 2.1-1 and 2.1-2). The air flow is powered by a 4.3-m diameter axial fan (Figure 2.1-3) directly driven by a.0.45MW electric motor. The 8 fan blades, which rotate at up to 600rpm are followed by a set of 53 stator vanes used to straighten the flow. Following the fan, the flow duct (of reinforced welded steel plate construction) transitions from a circular to a square cross-section 5.5-m on edge. In the air exchange tower the boundary layer is exhausted to atmosphere and replenished with new air injected tangentially through slots around the duct periphery. After two right angled corners, flow enters the 5.5 by 5.5-m settling chamber containing 7 anti-turbulence screens, but no honeycomb. The screens have a

60% open area ratio and are spaced at 15cm intervals. The 9:1 contraction downstream accelerates the flow to test speed and brings the duct dimensions down to the 1.85 by 1.85-m cross section of the test sections.

Both aerodynamic and acoustic test sections are 7.3-m in length and are of constant cross section, resulting in a slight favorable pressure gradient due to boundary layer growth of about 0.3% C_p per meter. Flow through the empty test sections is both closely uniform and of very low turbulence intensity. Table 2-1
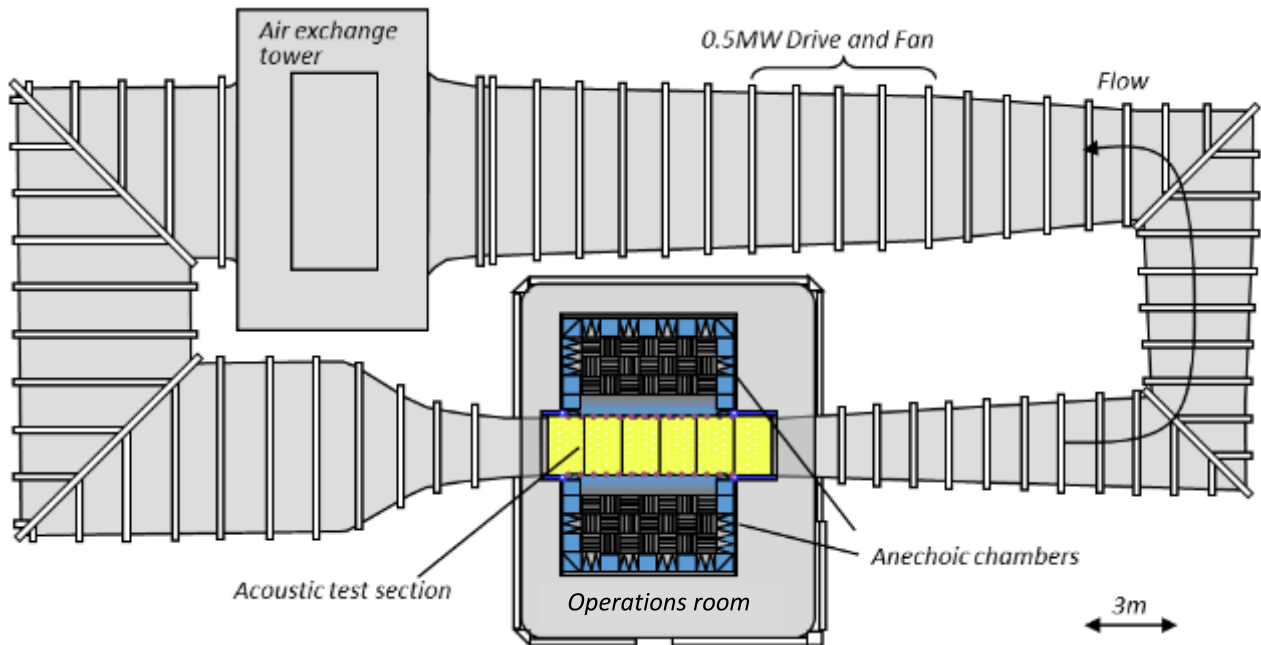

Figure 2.1-1: Plan view schematic of the Virginia Tech Stability Wind Tunnel with the hybrid anechoic test section and anechoic chambers installed.

Figure 2.1-2: View of the return circuit portion of the Virginia Tech Stability Tunnel, as seen from the right hand edge of Figure 2.1-1.

8-bladed 4.5-m diameter Clark Y fan (rotates counterclockwise)

53-bladed stator system 0.25m downstream of fan

Variable thickness Melamine liner designed to reduce tip gap and minimize tip gap variations

Figure 2.1-3: View of the 0.45MW fan at the Virginia Tech Stability Wind Tunnel from upstream.

shows 2006 measurements of free stream turbulence levels as a function of flow speed made in the hard-wall section. Turbulence levels are as low as 0.016% at 12m/s and increase gradually with flow speed. Choi and Simpson [7] measured the lateral integral scales of the streamwise velocity in both the horizontal L_z and vertical L_y directions. They found L_z=56mm for 15m/s and 28mm for 37.5m/s and L_y=122mm for 15m/s and 25mm for 37.5m/s.

Table 1-1: Turbulence levels in the empty test section of the Stability Wind Tunnel.

| Freestream Velocity U_∞ (m/s)	Turbulence Intensity u'/ U_∞
12	0.016%
21	0.021%
30	0.024%
48	0.029%
57	0.031%

Test section access door (closed during operation)   *Vortex generators*   *First turning vane set with access way open (closed for testing)*

25-mm thick Melamine foam thickening to 50mm near turning vanes

Figure 2.1-4: View of diffuser of the Virginia Tech Stability Wind Tunnel from upstream.

Flow leaving the test section enters a 3-degree diffuser (Figure 2.1-4). Four pairs of vortex generators mounted at the diffuser entrance are used to mix higher momentum flow into the duct corners to reduce the susceptibility of the flow to separation. Two further 90 degree corners, additional expansion of the duct and transition to a circular cross section return the flow to the fan. The four corners in the circuit are equipped with diagonal rows turning vanes spaced every 0.3 meters, except at the corner immediately upstream of the settling chamber where the spacing is 0.076 m.

Sting support

Turntable system for two-dimensional model mounting
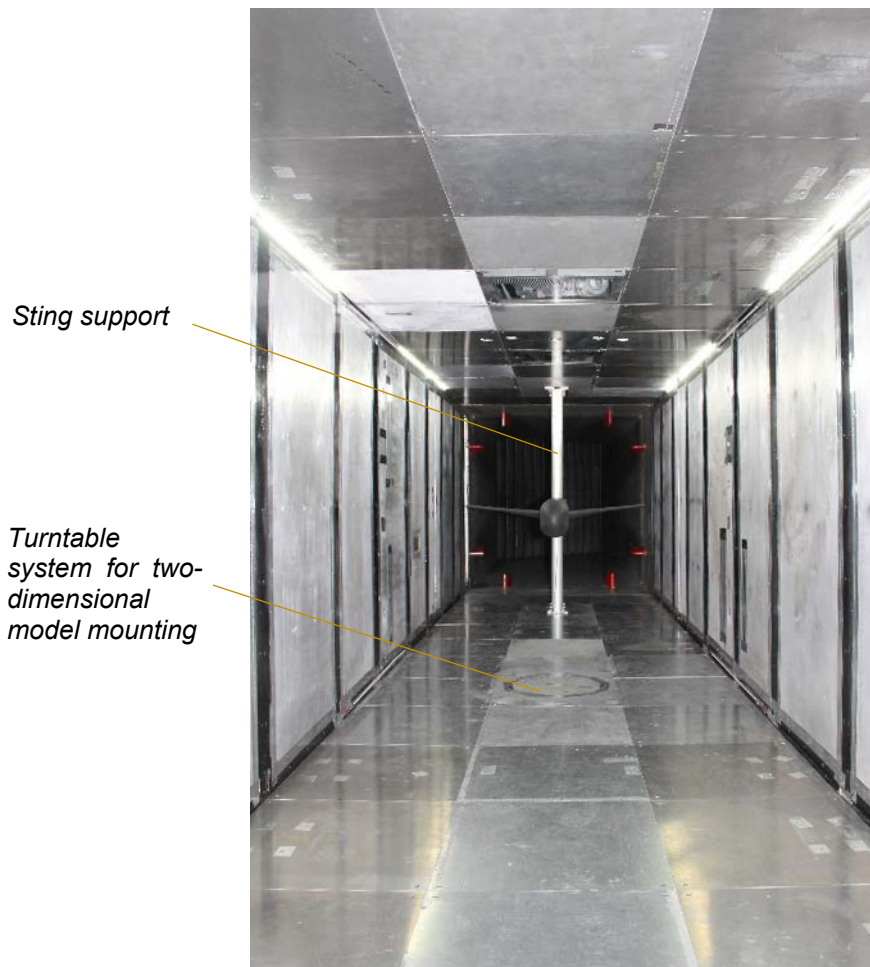
Figure 2.1-5: Hard-wall test section of the Virginia Tech Stability Tunnel with aluminum wall panels installed. View from upstream with an airplane model installed.

The test sections are housed in a large hermetically sealed reinforced-steel operations room (Figure 2.1-1 and 2.1-2). The pressure here is equalized with the static pressure in the test section flow, this being below atmospheric by an amount roughly equal to the dynamic pressure. The inside lower wall of the test section sits about 3-m above the operations-room floor allowing room for large models to be introduced to the test section through its floor. A clearance of about 2-m between the inside upper wall of the test section and the operations room ceiling allows space for a winch system used in model installation. The fact that the test section is accessible from outside greatly simplifies the operations and the placement of instrumentation, as well as permitting room for the anechoic system described below.

2.1.1   Hard-wall test section

All four walls of the hard-wall (or 'aerodynamic') test section (Figures 1-1 and 2.1-5) are hard surfaces. In its most common configuration, the side walls are formed from a sequence of aluminum panels that span nearly the full distance from floor to ceiling (Figure 2.1-5). The aluminum panels may be replaced by a matched set of Lexan panels when panoramic optical access is required. The panels are supported by a steel

structure that, on the inside of the test section, is flush with the panels creating smooth flow surfaces. The aluminum panels allow for rugged testing and easy installation of instrumentations. The floor and ceiling flow surfaces consist of an array of removable 0.61x0.61m aluminum or Lexan panels. The panels are aligned and accurately matched so as to produce continuous flow surfaces. They are also interchangeable with each other and with floor and ceiling panels from the acoustic test section, which have the same layout and position.

Two-dimensional models are mounted in the test section centered on an axis 3.56m downstream of the test section entrance. In the vicinity of the model support, two of the panels on the floor, and two on the ceiling (forming areas 0.61-m wide and 1.22-m long) are replaced with rectangular plates containing a circular turntable system that sits flush with both floor and ceiling (Figure 2.1-5). This system provides structural support for full-span models mounted vertically at the center of the test section. The turntable system is powered by a Kinematics model ZE14C slew drive under computer control that provides up to 1000Nm of torque, a rotation rate of 0.1rpm, and resolution of better than 0.01 degrees. Turntable position is sensed by a Renishaw LM10 linear magnetic encoder. Direct measurements of model position are made using four Acuity AR700-32 laser distance sensors installed in the aerodynamic test-section installed in the wind tunnel
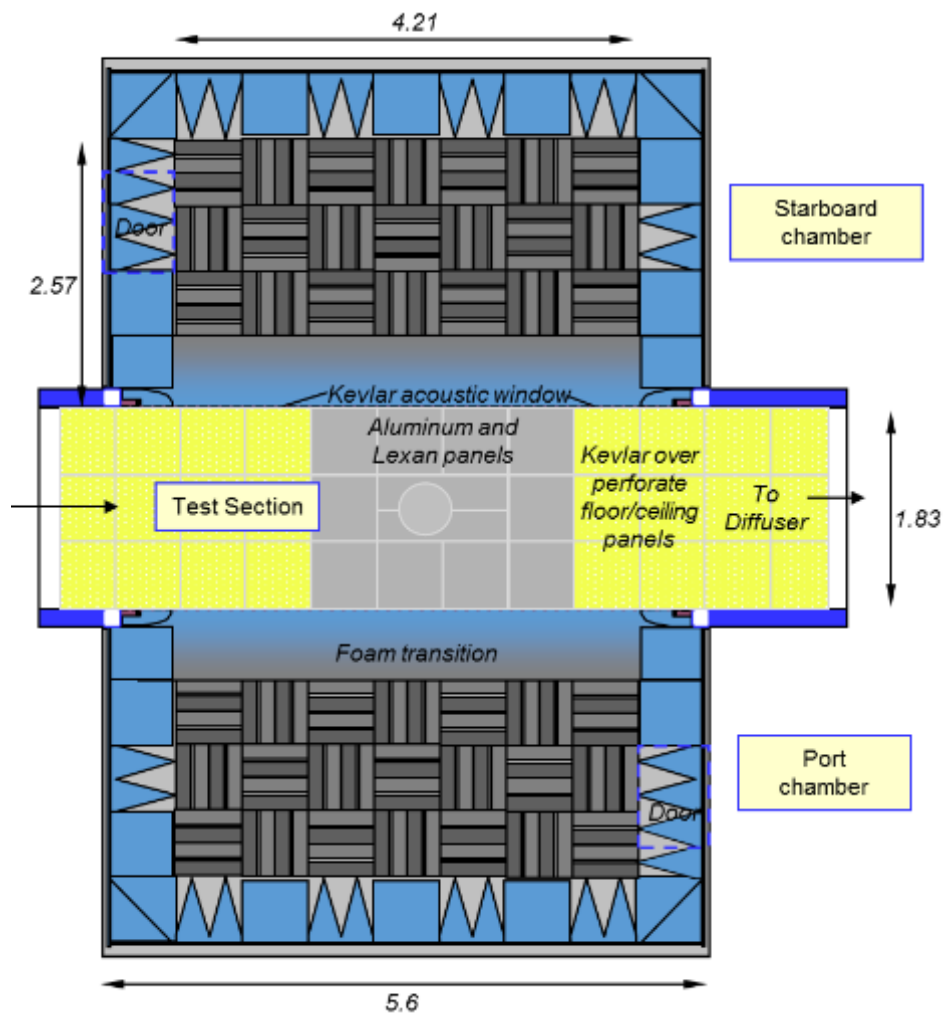

Figure 2.1-6. Plan view cross-section of the anechoic system as installed showing the test section flanked by the two anechoic chambers. Dimensions in meters.

walls, on either side of the model, and in the ceiling. A sting support, pictured in Figure 2.1-5, is also available.

2.1.2   Hybrid acoustic test section

The side walls of acoustic test section (Figure 2.1-3, 2.1-6 and 2.1-7) include 4.2-m long acoustic windows that span the full 1.85-m test section height. The windows are rectangular openings covered by tensioned Kevlar cloth that is transparent to sound and almost impervious to flow. Acoustically speaking the test section thus behaves as a half-open jet. Sound passes through the windows into two anechoic chambers that sit on either side of the section. The Kevlar acoustic windows eliminate the need for a colector and, by containing the flow, substantially reduce the lift interference compared to a free jet when airfoil models are placed in the test flow.

The flow surfaces on the upper and lower walls of the test section are formed primarily from the same Kevlar cloth used for the acoustic windows. The cloth, which forms a smooth, quiet, and acoustically transparent surface, is bonded to a series of 0.610-m square perforated aluminum panels that provide structural support, Figure 2.1-6. The panels are arranged 3-wide across the test section. The volume behind the panels is filled with 0.457m-high foam wedges that eliminate acoustic reflections at frequencies above 190Hz (Figure 2.1-7).

Models are mounted using a system that is a duplicate of that employed with the hard-wall test section, and at the same relative location as in the hard-wall test section (3.56m from the upstream end of the test section).
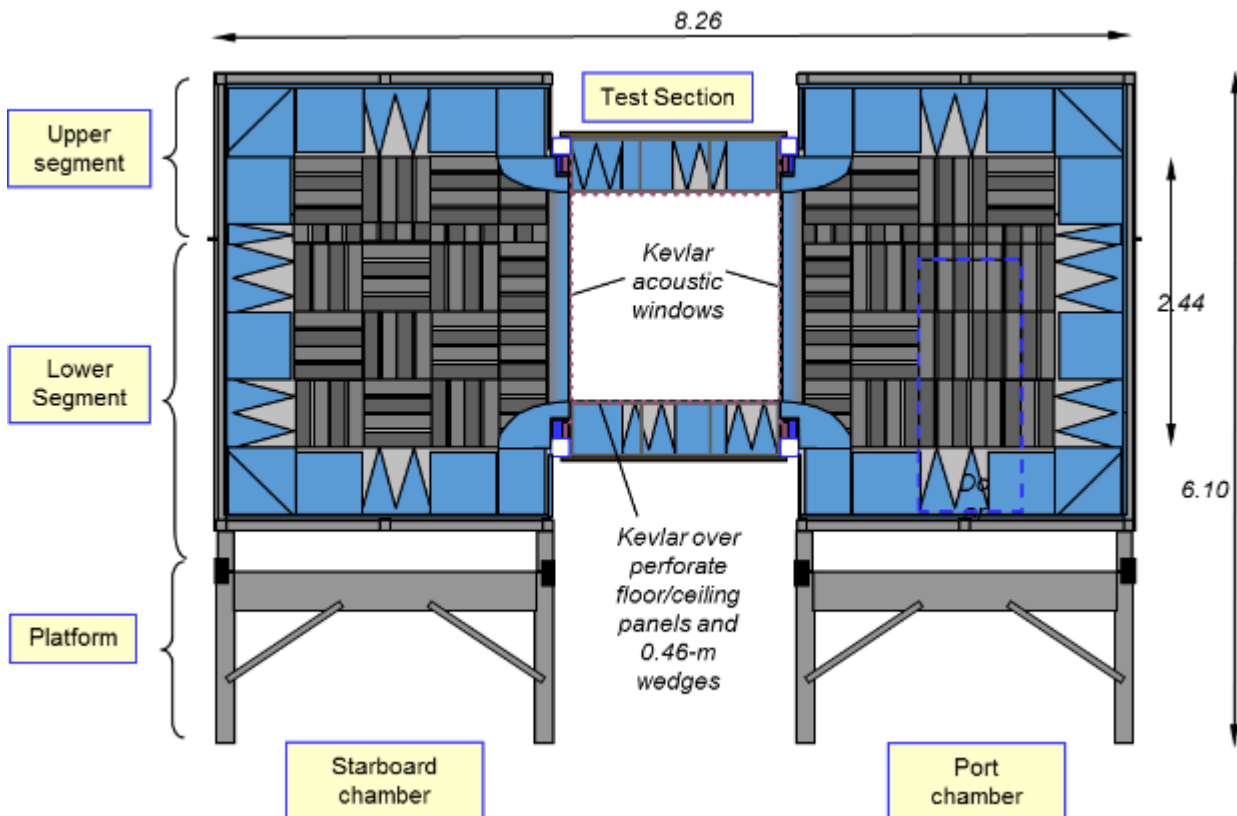

Figure 2.1-7. Cross section through the anechoic chambers and test section looking downstream. Dimensions in meters.

An identical circular turntable system, driven by a Kinematics model ZE14C slew drive, monitored by a Renishaw LM10 linear magnetic encoder system is used. Model position verification is performed using Acuity AR700-32 laser distance sensors installed in the anechoic test-section ceiling. Kevlar floor and ceiling panels around the model position may be exchanged with Lexan or aluminum versions to permit optical access or prevent parasitic noise generation, as described below.

Plain weave Kevlar 120 cloth is stretched on a 5.37x2.51m tensioning frame is used to form each of the acoustic windows. Two anechoic chambers are positioned on either side of the test section outside the anechoic windows (Figure 2.1-6 and Figure 2.1-7). Each chamber has a streamwise length of 5.6m, extends 3.2m out from the test section acoustic window, and has a height of 4.2m. The chambers walls are constructed from medium density fiberboard, supported by a network of external steel beams, and lined internally with 0.610-m high acoustic foam wedges that eliminate acoustic reflections at frequencies above 140Hz. Quarter-elliptical foam sections (Figure 1-2(b)) surround the acoustic windows so as to form a smooth transition between the lower and upper walls of the test section, on the inside of the windows, and the acoustically treated walls of the anechoic chambers on the outside of the acoustic windows. The chamber sections are designed to seal to the sides of the test section, though it is possible for some air to leak between the chambers through the acoustic treatment that forms the superstructure and substructure of the test section ceiling and floor.

2.2   The Poul la Cour Tunnel

Since the 1990's there has been an increasing need for wind tunnel tests to support wind turbine design. Especially there has been a need within design of wind turbine airfoils. In the start, aerodynamic tunnels were used, where there was only minor focus on the flow quality and no focus on the aeroacoustic characteristics. Since the size and thereby the investment in modern wind turbines are increasingly growing there is now big focus on both flow quality and the aeroacoustic characteristics.

DTU Wind Energy (formerly DTU and Risø National Laboratory) has for around 40 years carried out research in wind energy and supported wind turbine design and development. More specifically airfoil design and wind tunnel tests have been an ongoing activity for around 25 years. That was the reason that DTU Wind Energy observed a need for a wind energy dedicated wind tunnel and therefore proposed such an establishment of a wind tunnel as a national research infrastructure for the Danish Agency for Research and Innovation in 2010. After several months of dialogue in 2011 with the Danish stakeholders within wind energy (OEM's, research institutions and laboratories) a set of specifications were defined. Three different configurations of wind tunnels were investigated: 1) one dedicated aerodynamic and aeroacoustic tests of wind turbine airfoils, 2) one dedicated boundary layer flows and model wind turbine rotors and 3) one dedicated climatic conditions or a so-called "icing tunnel". The issues covered by all three concepts are important for wind energy applications. However, it turned out that the first priority among the stakeholders was a tunnel dedicated aerodynamic and aeroacoustic tests of wind turbine airfoils. One important aspect in the dialogue was the daily cost of the tunnel so the final specifications were balanced between the technical need and the corresponding cost. A project description for the wind tunnel establishment was submitted late 2011, and mid 2012 this project was granted by the Danish Agency for Research and Innovation. Thus, the starting point for this design was the specifications described below and a budget of around 10M€.

2.2.1   Specifications

The wind tunnel dedicated aerodynamic and aeroacoustic tests of wind turbine airfoils has the following overall specifications that is the basis for the airline design, see Table 2.2-1.

Table 2.2-1 Overall specification for the Poul la Cour Tunnel.

Description	Value
Maximum Reynolds number per meter [-]	7.0×10^6
Maximum flow speed [m/s]/[km/h]	~105/378
Test section: Width [m]	3.00
Test section: Height[m]	2.00
Test section: Length [m]	~9
Maximum turbulence intensity [%]	Max 0.1
Anechoic chamber: background noise at 60m/s with Kevlar walls 2m from airfoil [dB]	<70
Design flow speed for acoustic measurements [m/s]	60

Even though it is obvious that the specifications are crucial for the design process, it is very important to balance these specifications with the costs, because some of the requirements have more impact on the final cost than others. Whereas the specification of the Reynolds number is relatively easy to agree on, the requirement of the maximum turbulence intensity is not straight forward. However, a turbulence intensity of maximum 0.1% was chosen because measurements on full-scale wind turbines have shown a rather low turbulence intensity at the airfoil level. This turbulence intensity is much lower than normally measured in the atmosphere, where about 10% is normal. However, since the big vortices found in the atmosphere are omitted and not possible in a wind tunnel, and since the airfoils experience velocities that are up to nine times the wind speed, only the small vortices are observed. Designing for a turbulence intensity of 0.1% requires a relatively big contraction ratio that again requires a relatively long airline. Further to this, the requirements for relatively low noise require the use of noise absorption and materials, where vibrations are avoided. Thus, both the relatively long airline and the special noise absorbing and vibration free components increase the cost. When designing the Poul la Cour wind tunnel there was much focus on whether the different specifications were "need to have" or "nice to have" to balance the cost.

At the moment the Poul la Cour Tunnel is in construction and it is expected that it will be commissioned and run-in in early 2018. In Figure 2.2-1 a photo from March 2017 of the wind tunnel situated at the DTU Risø Campus, Denmark, is seen.

Figure 2.2-1. Photo of the Poul la Cour Wind Tunnel seen from south-west. Photo by Timm Becker.

2.2.2   Brief description of the tunnel

The tunnel is of the closed return type and has air exchange in the trailing edge of the test section, see Figure 2.2-2. The wind tunnel is dedicated tests on wind turbine airfoils and features three different test sections:

- a standard closed test section for two dimensional tests of airfoils,
- a hybrid anechoic test section for two dimensional tests of airfoils and,
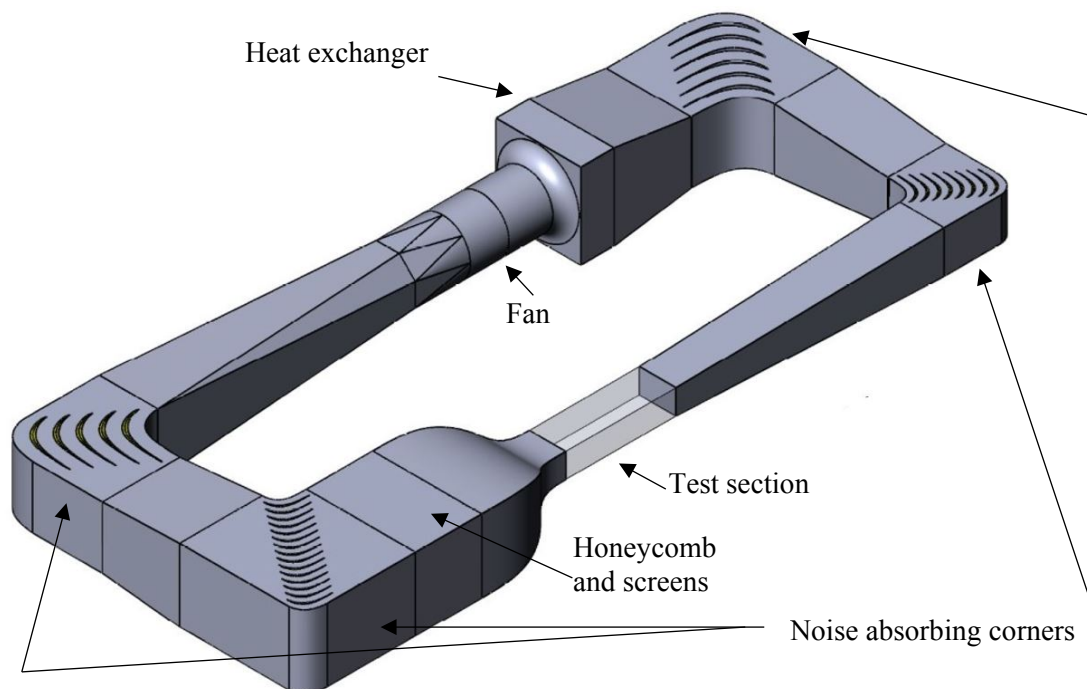- an open test section that will be used for acoustic tests, model rotors, bluff body tests etc.

Figure 2.2-2. Drawing of the Poul la Cour Tunnel.

The Poul la Cour Tunnel is designed with the following properties:

- guide vanes used as sound absorbing baffles in all corners
- expanding corners
- buffeting alleviation by use of a step in the cross section area upstream of the fan
- heat exchanger just upstream of the step into the fan
- contraction ratio 9 of test section nozzle
- no wide angle diffuser
- sound absorbing treatments in the fan walls and center body and parts of the airline
- anechoic room around the test section
- adapted for open, closed and hybrid anechoic test section

The air flow is driven by a 4.7-m diameter axial fan with a 2.4MW electric motor. The 16 fan blades rotating up to about 450rpm are followed by 10 stator vanes to ensure that the wake of each blade does not pass a stator vane at the same time. The fan is placed opposite of the test section to increase the distance from this noise source to the measurement position. The air line that is constructed primarily in concrete to dampen vibrations and noise from outside has four rectangular corners. In each of the corner the guide vanes direct the flow, but to meet the requirements for the acoustics in the test section the guide vanes in all corners are also designed to work as sound absorbing baffles (panel absorbers). With perforated steel plates forming the

guide vane surface, the absorption material made of mineral wool is inside each guide vane. The guide vanes closest to the fan have big chord lengths of 5.5m absorbing the lower frequencies, whereas the guide vanes closest to the test section have shorter chord lengths of 3.0m absorbing the slightly higher frequencies. Also, the tunnel circuit is designed using expanding corners to achieve the smallest possible footprint and thereby keeping the costs down. The expansion ratio is 1.32 in all corners. The heat exchanger is placed between the fan and the corner upstream of the fan for two reasons. First, the self-induced noise generated by the heat exchanger has to pass two corners before reaching the test section. This is good for the noise level in the test section. Second, the concept of designing the airline circuit with a large step in area before the fan, that has been utilized by the Japanese Railway Institute [38] and the rebuilt tunnel NWB [39] with success, makes it possible and also advantageous to place the heat exchanger just upstream of the fan and use it to dampen the acoustic waves in the situation of buffeting. Upstream of the test section the settling chamber holds one sheet of honeycomb and three screens. Because of the high requirements to the flow quality the contraction ratio is 9:1 and the flow is accelerated to the test section up to 105m/s. The big contraction ratio implies a larger tunnel, but is also more efficient since the losses in the flow conditioning elements will be smaller. Further details about the wind tunnel design can be found in Chapter 3.

3.0   OVERALL FACILITY DESIGN

Most wind tunnels focus on the flow characteristics so that further knowledge in a specific area can be provided. However, it is less common for tunnels to have a focus on both the flow characteristics and acoustic characteristics. Since the main volume of wind tunnels only focus on the flow characteristics there is a potential in rebuilding existing tunnels to obtain good acoustic characteristics. However, designing wind tunnels from scratch provide more degrees of freedom in the final design. In this chapter the design process for a new wind tunnel, the Poul la Cour Tunnel, and rebuilding an existing wind tunnel, the Virginia Tech Stability Tunnel, are described.

### 3.1   New facility design: The Poul la Cour Tunnel

The design of the Poul la Cour Tunnel was based on the specifications stated in Table 2.2-1. However, based on the specifications there are several solutions. Apart from the above specifications, other issues are important for design, including:

- Is possibility for testing at all times important? Or is it acceptable not to test when e.g. the outdoor humidity is high? This will give an answer to whether to choose an airline of the open or closed return type.
- Is it important to test with constant temperature? This will give an answer to whether a heat exchanger is needed and to whether a closed return type tunnel is needed.
- Will tests be carried out in an open or closed test section? If tests in an open test section will be carried out, the risk of buffeting should be considered carefully.
- Which noise level is the target? The target spectrum should be considered. It is especially important how much effort should be put on the lower or higher frequencies, because damping of low frequencies is somewhat more challenging than damping of high frequencies.
- Are damping of vibrations and outdoor noise important? This will be important for the decision of the choice of material for the airline, since it can be made of wood, steel or concrete.
- Will there be a hall to place the tunnel? This will also be important for the decision of the choice of material for the airline and if the dimensions of the hall will be a constraint to the airline design.

In the case of the Poul la Cour Tunnel it was clear that:

- Testing should be possible at all times because it should also support industrial purposes. That was one reason that an airline of the closed return type was chosen. A closed return type is also an advantage for the control of noise and temperature.
- A constant temperature is needed. This is because acoustic measurements will be carried out.
- Tests will mainly be carried out in a closed test section, but it should also be possible to carry out tests in an open test section. Therefore, buffeting should be avoided if possible.
- The noise level in an otherwise empty tunnel should be as low as possible compared to the trailing edge noise of an airfoil. In practice the target noise level was selected so that the background noise level around 1000Hz is at the same level as the trailing edge noise level, but where the background noise level above and below 1000Hz will be somewhat higher. This is to reduce the otherwise very high demands to the noise absorption.
- Damping from the fan and outdoor noise is important and therefore the airline should be built of concrete.
- There will be no hall around the airline, so the climate should be taken into account in the design and construction of the tunnel. Use of concrete will be an advantage for weather protection.

The design of the tunnel was divided into subcomponents, where the drag and noise absorption from each subcomponent wa computed. The subcomponents are reflected in the sketch below, Figure 3.1-1.
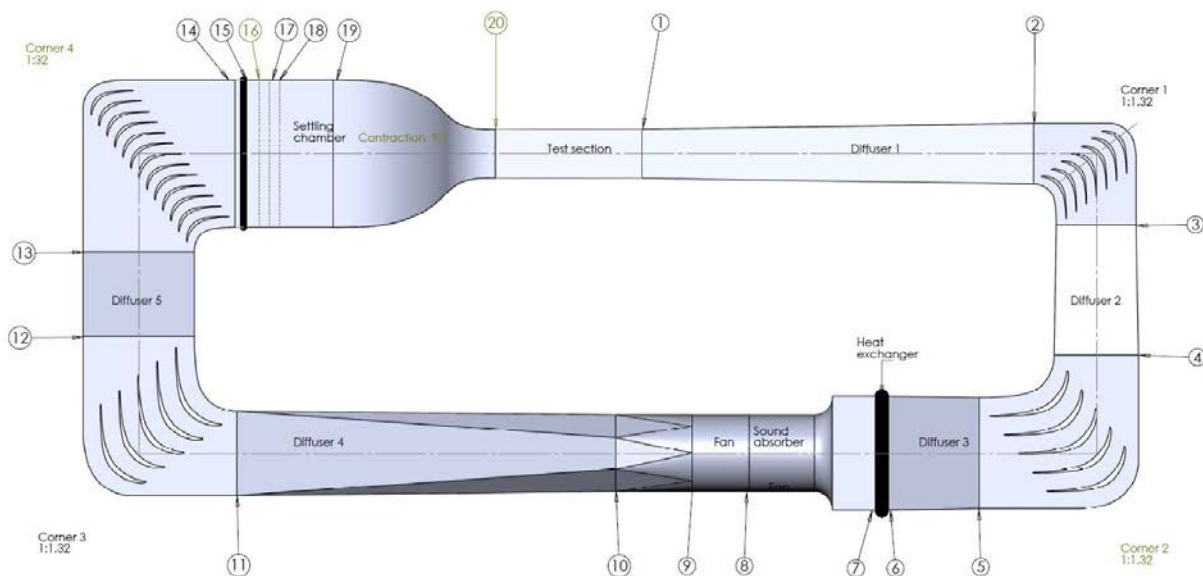
Figure 3.1-1   Sketch of a wind tunnel high lighting the sub components

- Test section (20 →1)
- Diffusers (Diffuser 1: 1→2, Diffuser 2: 3→4, Diffuser 3: 5→6, Diffuser 4: 10→11, Diffuser 5: 12→13)
- Corners (Corner 1: 2→3, Corner 2: 4→5, Corner 3: 11→12, Corner 4: 13→14)
- Heat exchanger (6→7)
- Sound absorbers (7→8, 9→10)
- Fan (8→9)
- Settling chamber (14→19)
- Contraction (19→20)
- Honeycomb (15)
- Screens (Screen 1: 16, Screen 2: 17, Screen 3: 18)

In the following, the design of the tunnel and each of the sub components are described.

3.1.1   Aerodynamic design

In the aerodynamic design there was a focus on the efficiency so as to reduce the power requirement for the fan, for two reasons. One reason was that, in general, the lower the needed power for the fan, the lower the emission of noise from the propeller. The other reason was that the operational cost for power will be lower. Apart from the efficiency, also the flow quality in terms of low turbulence and high uniformity was in focus because it is of key importance to obtain low turbulence intensity in the inflow. With the efficiency and the flow quality in mind the aerodynamic design was carried out.

3.1.1.1 Diffusers

There are five diffusers in the airline. Careful design of the diffusers is important for both keeping the tunnel losses down and for the flow quality of the tunnel. Since the velocity at the working section is high (up to 105m/s), the first diffuser normally amounts for a large part of the tunnel total losses. It is therefore especially important to optimize the operation of diffuser 1 carefully. High efficiency of a diffuser is normally linked to a relatively large expansion ratio with areas of separated flow. Charts from ESDU-73024 [32] show data for the flow regimes for conical diffusers as obtained through experiments. Dashed lines show the border between attached flow and separated flow. Since the inflow to diffuser 1 from the test section may be disturbed by, e.g. a stalling or highly loaded model, it may cause the diffuser to stall and to induce large flow disturbances all around the wind tunnel circuit. The design point needs to be made so that the flow is attached in the diffuser. Thus, diffuser 1 was designed with a margin to the stall boundary, thereby reducing the risk of stall in the diffuser.

When designing diffuser 2, 3 and 5 flow regimes for planar diffusers, ESDU-74015 [33] was investigated because these diffusers were single plane expansion diffusers or approximately of this type. The design point is placed so that attached flow is to be expected. However, since the diffuser cross section aspect ratio is close to one, it can be questioned whether the flow in the diffusers are two dimensional. The boundary layer on the side walls will add to the friction losses and may increase the tendency for separations in the corners. If the diffuser instead is treated like an equivalent conical diffuser, the theory behind this can be used to analyze the performance. The conclusion largely remains same, that the flow is attached within a good margin but the efficiency is slightly lower. The data from ESDU for planar diffusers was used in the performance calculation.

3.1.1.2 Corners

A guide vane profile optimized for use in wind tunnels with expanding corners is used. It was designed at the Royal Institute of Technology (KTH) by Lindgren *et al*. [34] following the work of Sahlin and Johansson [35] who designed a guide vane optimized for non-expanding corners with very low drag, for the minimum turbulence level (MTL) wind tunnel at KTH [36]. The expanding guide vane was designed through use of the MISES CFD code, see Drela and Giles [37]. The performance was experimentally verified in a series of experiments at KTH and has been used in several wind tunnel designs. The expansion ratio of the corners is 1.32. Since the guide vanes are also used as sound absorbing baffles with an unknown surface roughness, the drag was multiplied by a factor 2 in the performance calculation compared to the smooth surface to account for the unknown additional drag. It is very important that the guide vanes are designed to prevent any internal flow in the sound absorbing material, or in gaps that might occur between the material and the perforated sheet metal skin. Internal flow may severely degrade the performance of the guide vane. In Table 3.1-1 an overview of the guide vane design in the airline is seen.

Table 3.1-1 Corner configuration summary

Corner	Chord [m]	No of vanes
1	3.0	7
2	5.5	5
3	5.5	5
4	3.0	13

3.1.1.3 Heat exchanger

The function of the heat exchanger is to cool the wind tunnel air an amount (ΔT) equal to the temperature rise generated by the fan. Since the building material is concrete the heat exchange through the tunnel walls is negligible and the resulting cooling capacity must equal the fan power. Regarding the placement in the tunnel airline there exist two arguments for mounting the heat exchanger just upstream from the fan. First, flow generated noise from the heat exchanger has to pass two corners acting as sound absorbing baffles on both the up and downstream path before reaching the test section. Second, if placed at the optimal location in the tunnel, circuit calculations shown in section 3.1.2.4 below indicate that the resistance to the acoustic flow can work together with acoustic impedance step to remove buffeting. This concept is also utilized by the Japanese Railway Institute [38] and the rebuilt tunnel NWB [39].

The cross section area is 7m x 7m = 49m^2 at the heat exchanger. This gives a local velocity of 12.9 m/s at the maximum speed of 105 m/s in the test section. Primary aerodynamic design considerations for the heat exchanger are:
- local air velocity
- air pressure loss
- cooling capacity
- downstream temperature uniformity
- downstream turbulence

From existing wind tunnels the conclusion can be drawn that a minimum air-side pressure loss and turbulence generation can be best achieved by the use of a plate finned elliptical tube heat exchanger configuration. Any in-flow support structures should be kept at a minimum to reduce air flow blockage and have rounded leading edge and tapered trailing edge extensions. If the tunnel is operated when the relative humidity is high, condensation may occur in the heat exchanger. This is mainly a problem in the summer months. The condensation water must be collected and drained to prevent corrosion that otherwise might occur.

3.1.1.4 Fan

The fan design is carried out by a fan supplier, but general remarks, regarding a low noise fan suitable for this tunnel design, can be made:
- It is an axial fan
- It has an internal motor
- It has a relatively low rpm and thereby relatively high solidity
- It has well designed rotor and stator blades avoiding separating flow, vibrations and resonances.
- Have a stable mount isolating vibrations from the rest of the tunnel circuit.

The diameter of the required fan is 4.7 m. The hub diameter is 56% of the fan diameter and the fan efficiency is 0.89. The maximum electrical power is 2.4MW.

3.1.1.5 Honeycomb

The honeycomb effectively reduces disturbances in the settling chamber transverse direction of the flow but is not equally effective to reduce streamwise disturbances. For the honeycomb to function properly it is of great importance that the aspect ratio of the cells is large enough, at least 10. The honeycomb used in the tunnel has a $L/D_h = 16$. Two concepts exist for the honeycomb:

1. A continuous honeycomb in stainless steel, sometimes manufactured in place.
2. An assembly of honeycomb blocks, usually from aluminum, mounted on pretensioned steel bands.

It is recommended to use a honeycomb manufactured in one piece, if possible, to avoid disturbances from joints. However, a challenge with one piece is that large deflections might be a result and that the honeycomb therefore is not aligned with the flow. Therefore, the honeycomb is assembled from relatively few blocks, that is nine, with a size of approximately 3m x 2m, to minimize disturbances from the joints. The cells in the honeycomb have a diameter of 9.5 mm, the cell length is 152 mm, the cell wall thickness is 0.127 mm and the material is stainless steel.

3.1.1.6 Screens

The screens are most effective in damping out irregularities in the streamwise velocity but also damp lateral flow component irregularities to a smaller extent. In this process the flow through the screens results in a lateral redistribution of the flow. Therefore, a combination of screens and a flow straightener (honeycomb) to decrease variations in flow angularity has been successfully applied in many wind tunnel designs. Ideally, the flow straightener should be late in the series of flow conditioning devices but in practice it is very difficult to manufacture and mount the flow straightener with the accuracy that is needed. It is relatively easier to obtain high quality screens. Also, for larger tunnels the flow straightener usually has to be assembled from smaller pieces with joints causing flow disturbances. Therefore, the usual practice is to mount the flow straightener first. The least pressure drop for a given turbulence reduction is achieved when using a series of screens starting with the coarsest and continue to add finer and finer screens, see Groth and Johansson [40]. The screen porosity is defined as $\beta = (1 – d/M)^2$, where d is the wire diameter and M is the mesh width. The porosity β should not be smaller than about 0.55 to avoid jet coalescence resulting in large disturbances. For screens 1,2 and 3 d is 0.71mm, 0.56mm and 0.16mm, M is 3.2mm, 2.4mm and 0.7mm and β is 0.61, 0.59 and 0.60.

3.1.1.7 Settling chamber

The settling chamber is in this tunnel a 4 m long straight section downstream of the last screen. This allows residual turbulence to decay before entering the nozzle and is important to achieve a low turbulence level in the test section.

3.1.1.8 Contraction

The contraction geometry was designed at the Department of Mechanics (KTH) for the MTL wind tunnel using potential flow computations combined with boundary layer calculations, see Downie et al. [41]. The contraction is shown to be free from separation and has an excellent flow quality, Johansson [42] and Lindgren and Johansson [43].

3.1.2 Acoustic design

To create efficient sound absorption in the tunnel only the parts of the tunnel that contain noise treatments were considered. Placement of absorption material in narrow channels (baffles) is more efficient that in wider channels and the baffles can be designed with respect to length, thickness and distance between the baffles to create efficient noise reduction in the desired frequency range. In Figure 3.1-2 a sketch of the placement of the sound absorption in the tunnel is shown.
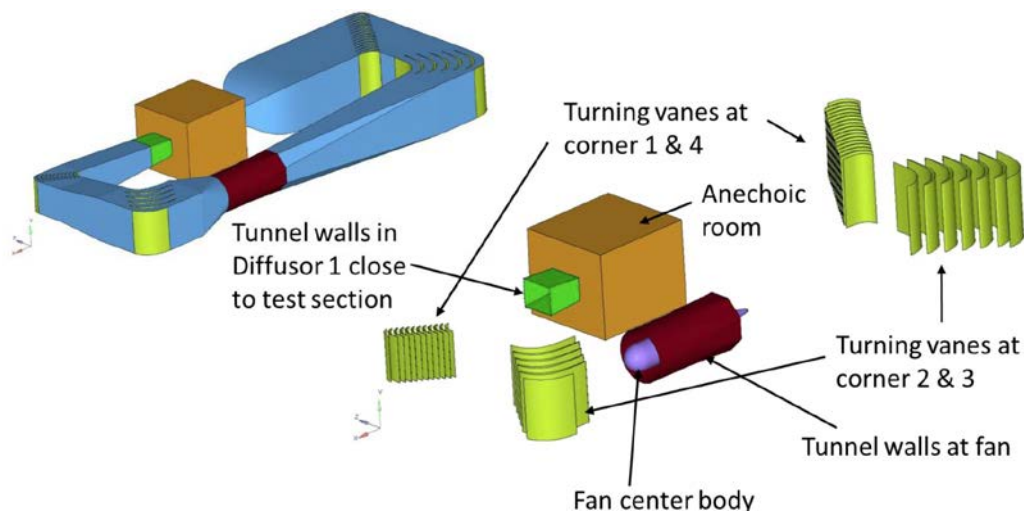
Figure 3.1-2   Sketch of placement of noise absorption elements in the Poul la Cour tunnel.

From the sketch it is seen that noise treatment is applied 1) in the corners, where guide vanes are mounted, 2) around the fan between the hub and the wall and 3) in the first part of diffuser 1 after the test section. The design of each of the elements is described below.

3.1.2.1 Corners

The guide vanes are designed as curved baffle silencers having a porous absorber on each side of the guide vane. A pressure-tight barrier is placed at the centerline of the vane and the outer surface is defined by a perforated panel. In-between those panels, porous absorptive material is placed. The porosity of the outer panels should be at least 30 %. Note that the tunnel walls at the corners have the same treatment as the corresponding guide vanes, that is, there must be space in the outer walls of the tunnel to include the porous absorber covering at least the same length as the guide vanes. The guide vanes provides excellent noise reduction in the frequency range where it works as a baffle silencer, but also provides high noise reduction above this frequency range due to the curved shape. In the simulations, the absorption material in the guide vanes is specified using the geometrical distribution of the material and a model for acoustic wave propagation in the porous material.

A two-dimensional model is derived for evaluating the noise level in the mid to high frequency range, see Figure 3.1-3. The model is derived only for the guide vanes and neglects the influence of the flow in the tunnel circuit. The finite element model of the guide vanes is derived with a maximum element size of 1 cm. With minimum 8 elements per wavelength, the model is valid up to 4500 Hz. An acoustic line source is applied at one end of the guide vane and free radiating boundary conditions are applied at the inlet and outlet of the guide vane corner model. The sound power level is determined before and after the guide vane and the insertion loss is predicted. The insertion loss is then used together with the noise data from the fan supplier to predict the noise level at the test section.

The insertion loss of the guide vanes is predicted in the frequency range from 50 Hz up to 4500 Hz. The 2D model focuses on frequencies above 300 Hz. The applied line source generates a pressure distribution in the investigated guide vane. The pressure level before and after the guide vane is then used to calculate the insertion loss. The predicted insertion loss versus frequency is presented for the four corners in Figure 3.1-4. The simplification of using a 2D model and a plane wave excitation can

be considered conservative. With a more random distribution of the acoustic waves impinging on the guide vanes, the insertion loss should not be reduced.
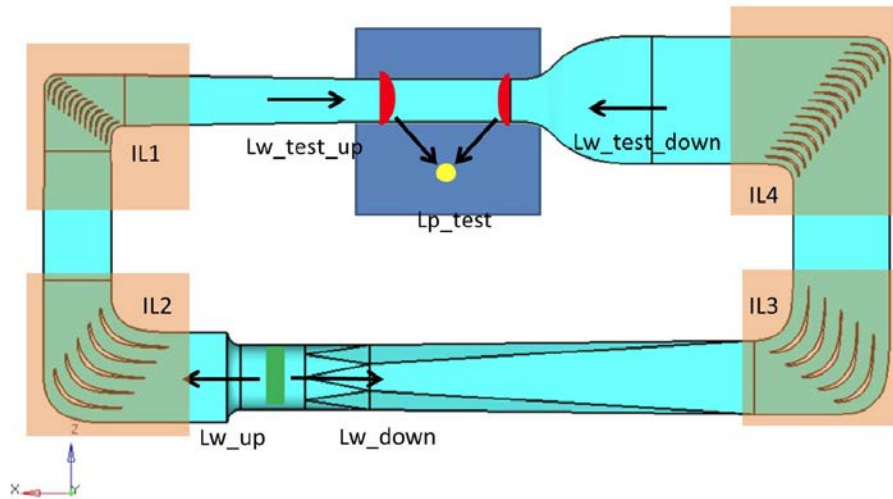
Figure 3.1-3   2D simulation model. The noise in the test section is predicted by subtracting the insertion loss in the guide vanes from the noise radiated from the fan.

To validate the simulations an experiment was carried out, where a downscaled guide vane with chord length 1.5m was tested in a laboratory in a duct made of MDF boards extending around 4m to each side of the corner. The guide vanes tested in the laboratory were manufactured with a surface of perforated steel plates with a porosity of 30%, where the holes had a hole diameter of 2mm. Inside the guide vane two different absorption materials were used: Polyester foam and mineral wool. The experiments showed that the simulations predicted the acoustic performance well and that the mineral wool was superior to the polyester foam in damping performance between 500Hz and 3000Hz. Thus, in the design of the guide vanes mineral wool was used as noise absorbing material.
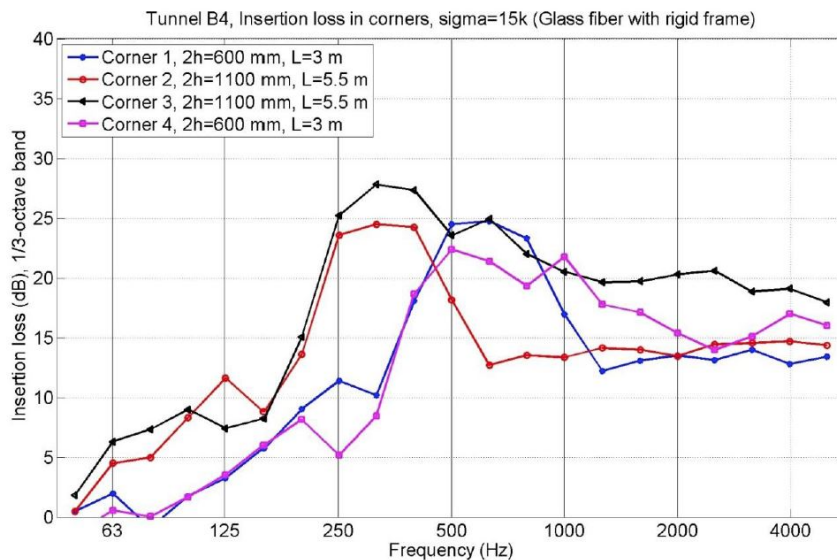
Figure 3.1-4   Insertion loss for each of the four guide vanes.

3.1.2.2 Fan and diffuser 1

The design of the silencers at the fan and the silencer in diffuser 1, close to the test section, is similar to the design of the guide vanes. The porous material is placed behind a perforated panel. A solid wall, typically constructed in steel or concrete, is placed behind the porous material. The thickness of these treatments are 0.4 m. Simulations in 2D similar to those carried out for the guide vanes are carried out for the silencers close to the fan and test section and the insertion loss for these silencers are presented in Figure 3.1-5.
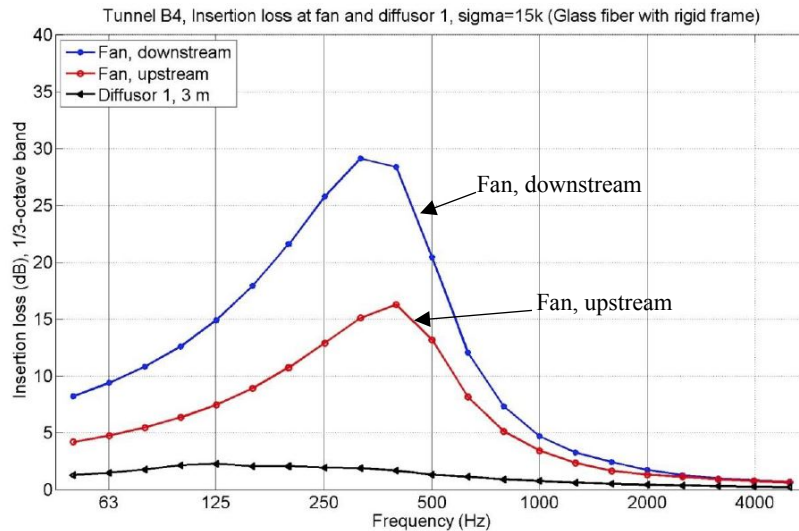
Figure 3.1-5   Insertion loss for the fan tail cone ("Fan, downstream"), fan nose cone ("Fan, upstream") and first part of diffuser ("Diffuser 1").

3.1.2.3 Overall noise absorption

The insertion loss in the upstream and downstream direction from the fan to the test section is presented in Figure 3.1-6. These predictions are based on 2D computations. In Figure 3.1-7 the predicted noise in the test section is presented based on the fan noise data from the suppliers and the predicted insertion loss in the guide vanes and silencers. It is seen that the target is more than reached for frequencies between 150Hz and 1200Hz and that the target for the other frequencies has been reached. However, the aerodynamic self noise that is not part of these predictions will change this picture somewhat.
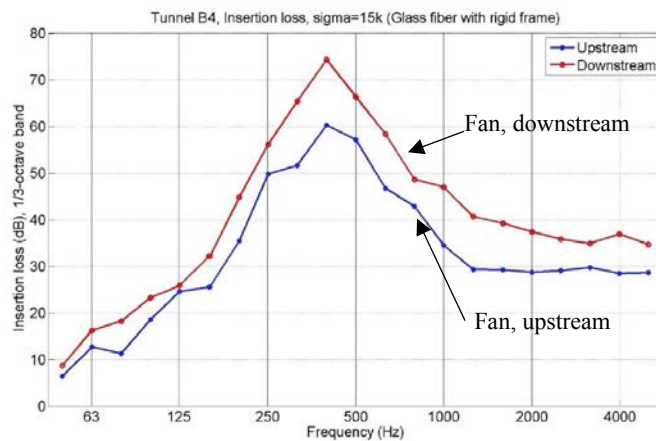

Figure 3.1-6   Total insertion loss: Upstream of fan (Nose cone, Corner 2, Corner 1 and diffuser 1) and downstream of fan (Tail cone, Corner 3 and Corner 4).
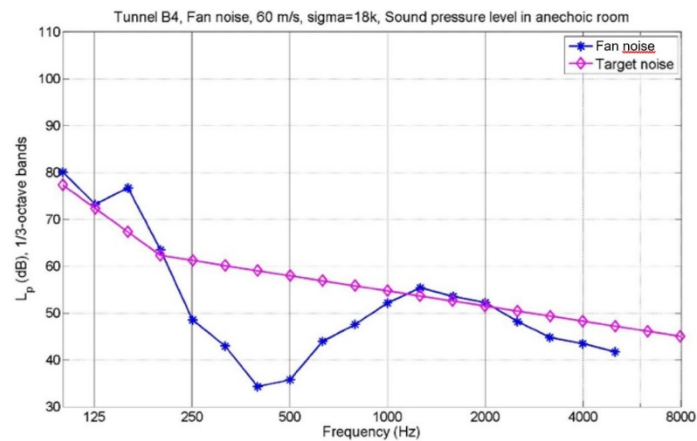
Figure 3.1-7   Fan noise in the test section with noise treatments.

3.1.2.4 Buffeting

Buffeting is an important issue when tests are carried out in an open test section, where vortices hitting the collector into the diffuser interacts with the lowest acoustic modes in the wind tunnel. This issue is important both in terms of acoustics, where the lowest modes of the acoustic waves can be violent, and aerodynamics, where e.g. drag measurements can be affected by the lowest modes. An evaluation of the risk for buffeting was carried out for the tunnel.

First, the lowest modes of the acoustic waves of the tunnel were derived. Here, the frequency response to a point source, placed at the collector in the test section, was evaluated in order to estimate the influence of the heat exchanger. The heat exchanger was modelled coarsely as a porous material introducing flow resistivity to reduce the peak response at the tunnel resonances. Modeling with and without a heat exchanger is seen in Figure 3.1-8, showing the acoustic response at the contraction for excitation at collector.

Second, the vortex shedding frequency for the tunnel was presented and compared to the natural frequencies of the acoustic modes for the tunnel. It appeared that the heat exchanger was influencing the peak levels in the frequency response between 4 Hz and 10 Hz. That is, the heat exchanger introduce damping to the acoustic modes. In Figure 3.1-8 distinct peaks are seen if no heat exchanger is installed and the suppression of the peaks are seen if a heat exchanger is installed. If vortex shedding frequencies match acoustic modal frequencies there will be a risk for buffeting, but to conclude it seems that the damping introduced by the heat exchanger can be a possible treatment to limit the buffeting issue.
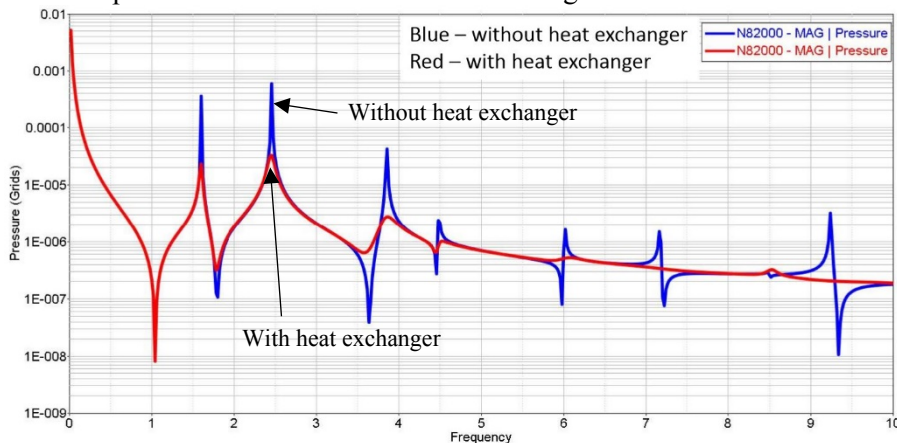

Figure 3.1-8   Buffeting: Acoustic response at contraction for excitation at collector

3.1.2.5 Design of the anechoic chamber

The basis for the design of the anechoic chamber was the requirement for acoustic tests down to a frequency of 100Hz. In contrast to traditional anechoic chambers some background noise will be present during the measurements, especially from the fan, and therefore a complete acoustic sealing of the chamber is less important compared to traditional chambers. The dimensions and especially the width of the chamber was given by the acoustic requirements, because the distance from the microphone array to the wind tunnel model and to the fibre wedges at the wall required a minimum distance. However, also requirements for crane operation and the possibility for changing configuration in the test section design constrained the height and length, respectively. The dimensions of the anechoic chamber was Length × Width × Height (L × W × H) equal to 13.0m×11.0m×11.55m. At the walls, the floor and the ceiling, mineral fiber wedges with a height of 0.85m will be mounted.

3.2 Considerations for retrofitting

The Stability Wind Tunnel was originally designed and constructed purely for aerodynamic work. Other subsequently retro-fitted facilities include the 2m Low Speed Wind Tunnel at JAXA [8]. Of course, many aspects of these conversions are facility specific, but in retrospect it is clear that certain characteristics make a facility more suitable as a candidate for conversion.

At the top of this list is test-section and facility configuration. The test section walls must permit the installation of flat tensioned cloth walls that form the acoustic windows. This favors a rectangular test section, though not exclusively – a Kevlar-walled test section has been installed in the 8-foot octagonal test section of the Anechoic Flow Facility at NSWCCD in Maryland [2]. The test section also needs to be long enough to take advantage of the acoustic benefits described in section 4.1. Interchangeable test sections are a great advantage if backwards compatibility to the original aerodynamic configuration is desired. A flow path that places the fan out of sight of the test section is important if parasitic noise sources from the fan (likely the dominant source) are to be managed.

Another critical requirement is space. While a hybrid anechoic test section can have the same interior dimensions as its aerodynamic counterpart, considerable exterior space is needed for one or more anechoic chambers and acoustic treatment. Typically, acoustic treatment will need to have a thickness of at least ¼ of a wavelength of the lowest frequency of sound to be absorbed. This is the minimum space requirement behind test section walls. For walls that will function as acoustic windows, additional space will be required for an anechoic chamber. At minimum, microphones in the chamber, will need to be placed at least ¼ of a wavelength away from the tops of acoustic wedges [2], sufficiently far from the model inside the test section so as to be in the acoustic far-field (at least one wavelength), and far enough from the exterior of the acoustic window to be outside the range of evanescent pressure fluctuations generated by the boundary layer growing on its interior surface. Assuming the lowest frequency of interest to be equal to the test section width, this implies *at minimum* space equivalent to the test section width outside the acoustic window. In practice, considerably more space than this is desirable to allow for flexibility in the placement of instrumentation and to accommodate the supporting structure of the anechoic chamber(s). A space-saving measure implemented at the JAXA 2m tunnel is to build a full anechoic chamber only on one side of the test section. The chamber on the other side is built only deep enough to contain the acoustic wedges and serves, effectively as an acoustic absorber.

The aerodynamic efficiency of the flow path is also important when considering upgrading from aerodynamic to aeroacoustic capability. Regions of flow separation in the circuit, poorly performing turning vanes, or a stalled diffuser, for example, all increase flow losses. These deficiencies increase the fan speed needed to maintain a given flow speed in the test section, with parasitic noise varying as the 6th power of the fan speed. For this reason, closed-circuit wind tunnels are more suitable as retrofit candidates than open circuit arrangements.
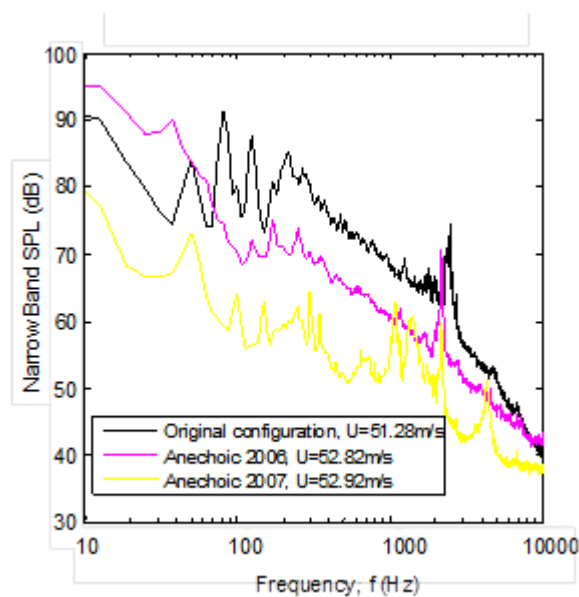
Figure 3.2-1. Inflow noise levels near the center of the test section at different stages of the development of the hybrid anechoic system for the VT Stability Wind Tunnel (from Remillieux *et al.*, 2008).

Correcting flow deficiencies can have a significant impact on sound levels, but background noise levels in the test section are bound to remain a concern for most retrofit projects. As with the VT Stability Tunnel non-acoustic tunnels are often fitted with fan systems not designed to be particularly quiet. The fan is likely the most expensive and embedded piece of the facility and thus logistically and financially difficult to replace. However, substantial acoustic improvements are possible. Figure 3.2-1 shows the progression of background acoustic levels near the center of the empty test section during the development of the hybrid anechoic arrangement for the VT Stability Tunnel [6]. The black line in this plot denotes sound levels in the hard-wall test section of the unaltered facility. The purple 2006 curve are measurements made after the first installation of the anechoic test section and chambers. Just opening the flow path has reduced sound levels by up to 5 to 10dB at frequencies above 100Hz. The further reductions across the frequency range, denoted by the yellow curve, to a total of as much as 25dB were the result of a sequence of improvements (note that much of this residual sound was generate by the microphone mount). These include, primarily, the application of 25-mm and 50-mm thick acoustically absorbing foam to the walls of the diffuser and settling chamber and the installation of a fan liner. The liner in its ultimate configuration (Figure 2.1-4) is not an acoustic absorber. It is merely a hard plastic fairing machined to circularize the duct surrounding the fan and reduce the tip gap.

4.0 TEST SECTION DESIGN

4.1 Test section layout

All hybrid anechoic tunnels to date have been based on a semi-anechoic configuration with a rigid test section ceiling and floor, and acoustically transparent side walls. On can certainly envisage other configurations, particularly for small facilities, such as the fully anechoic concept illustrated in Figure 4.1-1. However, for large facilities model mounting and personnel access requirements quickly constrain the design, strongly favoring configurations with at least a rigid (though potentially sound absorbent) floor.

Since aerodynamic corrections for a semi-anechoic hybrid test section are similar in magnitude to those of hard-wall test sections[9], the sizing of the cross-section of the test section can be based upon the same considerations of overall blockage, desired model aspect ratio (for two-dimensional testing), and sufficient test
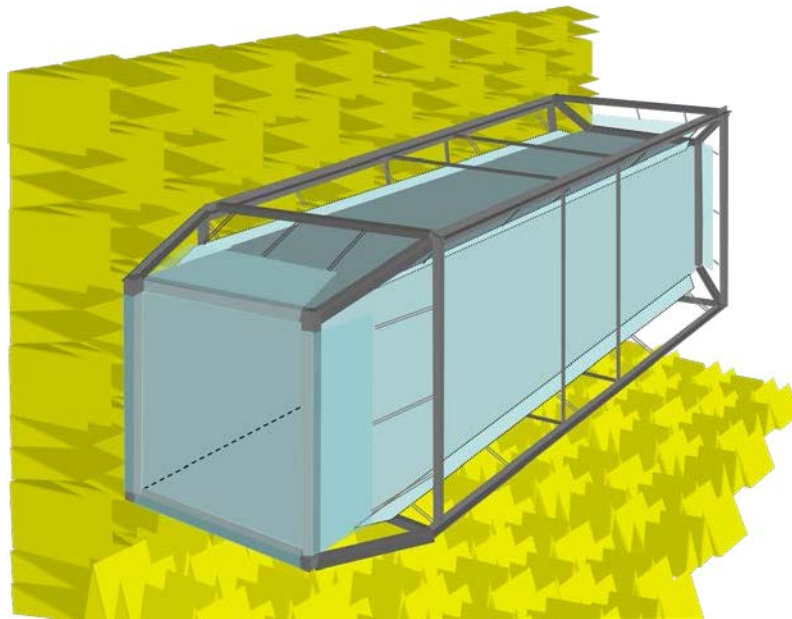
Figure 4.1-1. An early (2003) concept for a fully anechoic tensioned Kevlar test section.

Figure 4.1-2. The VT Stability Tunnel in hemi-anechoic configuration. The transparent wall on the right is used to grow a thick turbulent boundary layer ingested into the rotor system shown. The transparent wall replaces the starboard side acoustic window.

section length for parallel flow ahead and downstream of the model that drive aerodynamic test section design. At the VT Stability Tunnel we have found that two-dimensional models with chordlengths up to half the test section width (in the lift direction) can be tested up through stall without compromising aerodynamic accuracy.

A semi-anechoic test section configuration is also easily converted to 'hemi-anechoic' by replacing one of the acoustic windows with a rigid surface. This can be advantageous for the study of boundary layer related

aeroacoustics, since the rigid wall can then be used to grow high Reynolds number boundary layers. Figure 4.1-2 shows one such application where the aeroacoustics of a propulsion rotor in the presence of inflow distortion generated by a thick turbulent boundary layer are under study.

Acoustically speaking, one of the major advantages of the hybrid configuration is that the elimination of the jet and collector allow for a much longer test section. This not only increases the range of streamwise directivity angles at which noise measurements can be made from outside the test section, but also has a substantial effect on improving the signal to noise ratio and low-frequency resolution of measurements made using microphone phased arrays. Figure 4.1-3 illustrates this effect. An array of aperture D is place at a distance s from a model at the center of a hybrid test section. The spot size of a source of interest, generated by the model will be proportional to s and the acoustic wavelength λ, and inversely proportional to D. Indeed for a typical array with a significant number of microphones (e.g. a 40 microphone spiral array) the spot size radius $R_s \approx 0.6\lambda s/D$. Here, if we define the radius as extending from the spot center to the point where the array response is 3dB down. At the same time, the sound measurement is contaminated by parasitic noise coming from the rest of the tunnel circuit. This noise will appear as sources at the ends of the test section with image radius R_n. The greater the length of the test section L compared to its width h, the longer the length of the region around the model L_{eff} where the acoustic image will be free of parasitic noise contamination. Now, $L_{eff} = 2s \tan \theta - 2R_n$ where θ is the angle subtended by the test section ends to the array normal. Therefore

(4.1)

$$\frac{L_{eff}}{2R_s} \approx \frac{D}{0.6\lambda} \tan \theta - \frac{R_n}{R_s}$$

The acoustic image is usable only if $L_{eff}/2R_s > 1$ and this occurs when

(4.2)

$$\frac{D}{\lambda} > 0.6 \frac{1 + R_n/R_s}{\tan \theta}$$

Thus increasing the length of the test section, and therefore θ, extends range of feasible sound measurements to lower frequencies.
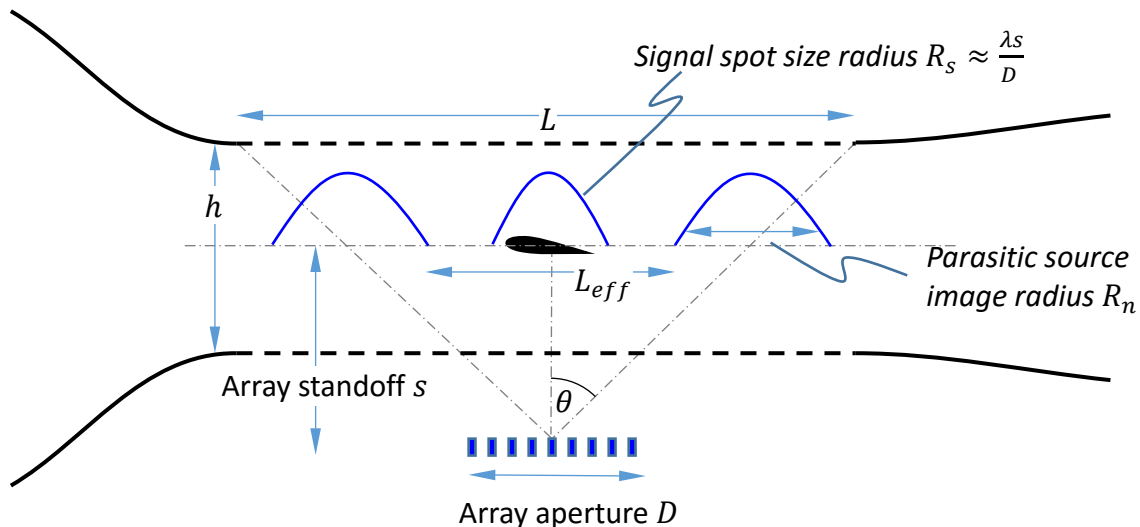

Figure 4.1-3. Beam-forming in a hybrid test section.

Of course, extending the test section length also reduces the intensity of the parasitic sources compared to the signal of interest by the inverse square of the free propagation distance, and therefore as $\cos^2 \theta$. Ignoring this effect, and differences in the parasitic and model source strengths, the parasitic source image size R will be greater than the signal image R_s because it is a factor $1/\cos\theta$ further away, and because the effective aperture of the array in its direction is $D/\cos\theta$ we would have $R_n = R_s/\cos^2\theta$. Substituting this into equation 3.2 we obtain,

(4.3)

$$\frac{D}{\lambda} > 0.6 \frac{1 + \sec^2 \theta}{\tan \theta} \approx \frac{1.2}{\theta} + \cdots$$

where the leading order expansion is reasonably accurate for θ (in radians) up to about $\pi/6$, beyond which this function starts to grow. However, this growth is a consequence of ignoring the propagation distance effect. Incorporating that effect and assuming the parasitic and model source strengths are the same, the $1.2/\theta$ rule of thumb remains accurate over about the same range and gives a conservative estimate of the benefits of increasing the test section length beyond that.

As an example, in the Virginia Tech Stability Wind Tunnel which has a 4.2-m long and 1.85-m wide acoustically transparent section, we have used a 1.1-m diameter spiral array with a standoff distance from the test section centerline of 1.6 m (placing the array just under 0.7-m from the nearest Kevlar wall is easily sufficient to avoid any near field pressure fluctuations from the test section boundary layer). This implies $\theta \approx 0.69$ radians or close to 40 degrees. Thus, $D/\lambda \approx 1.7$ and we would expect the lowest frequency at which the sound from a centrally placed model would be distinguishable from facility noise of similar strength to be about 540Hz using conventional delay and sum beamforming, quite close to that observed in practice. Of course, increasing the array aperture, reducing the facility noise (where possible) or using a deconvolution algorithm will potentially lower this limit further.

Another example is the test section in the Poul la Cour Tunnel that conceptually is slightly different because the pressure in the test section is equal to the atmospheric pressure and because the test section is centered in the anechoic chamber. Apart from this difference the test section with cross sectional area of 2.0m×3.0m is similar to the Virginia Tech Stability Wind Tunnel. The test section is 9.0m long and 6.0m of the walls on
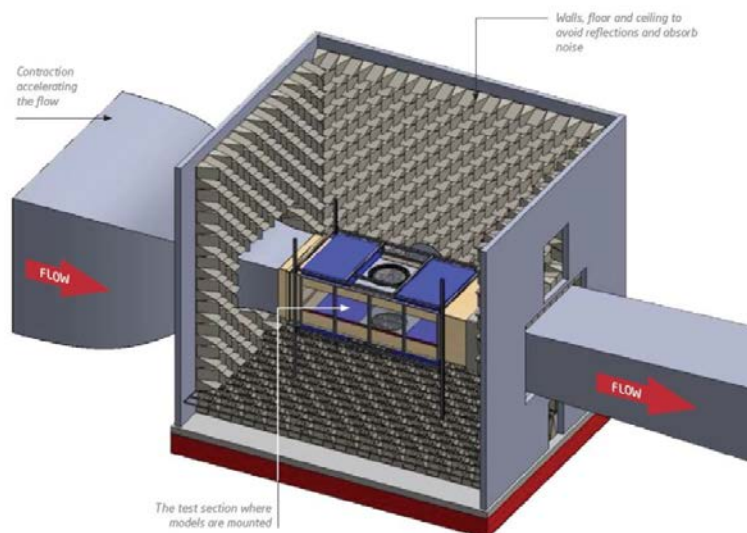

Figure 4.1-4   Drawing of the anechoic chamber including the hard wall test section in the Poul la Cour Tunnel.

each side of the test section are exchangeable. Thus, in one configuration the walls, ceiling and floor are hard and made of patches of wooden plates and acrylic glass and in another configuration the walls are made of Kevlar and the ceiling and roof have a perforated surface with acoustic absorption behind. In the middle of the test section an airfoil is vertically mounted in a pitch bearing, where the pitch angle are controlled by a servomotor driving a gear on a toothed wheel. This way the pitch can be controlled with high precision. In the Kevlar configuration a microphone array is mounted in the anechoic room in the same way as in the Virginia Tech Stability Wind Tunnel, which is about 0.5m from the Kevlar window and thereby about 2m from the airfoil. Since measurements should also imply low frequencies down to 300Hz, the microphone array needs to be relatively big. Therefore, the microphone array has a diameter of 2m. In Figure 4.1-4 a drawing of the test section in the Poul la Cour Tunnel is seen.

4.2 Design of the acoustic windows

The concept of replacing test section walls with tensioned acoustically transparent membranes is straightforward. Implementing this concept in practice involves a number of details, the most important of which are outlined here.

Obtaining Kevlar 120 scrim is not difficult. This material is readily available from manufacturers such as Hexcel who supply this for use in composites. However, it is rarely stocked in widths over 1.5-m, which are needed for larger wind tunnel applications. (A margin of about half a meter of Kevlar material is needed beyond the edges of the window in larger applications to enable mounting and tensioning.) One option is to
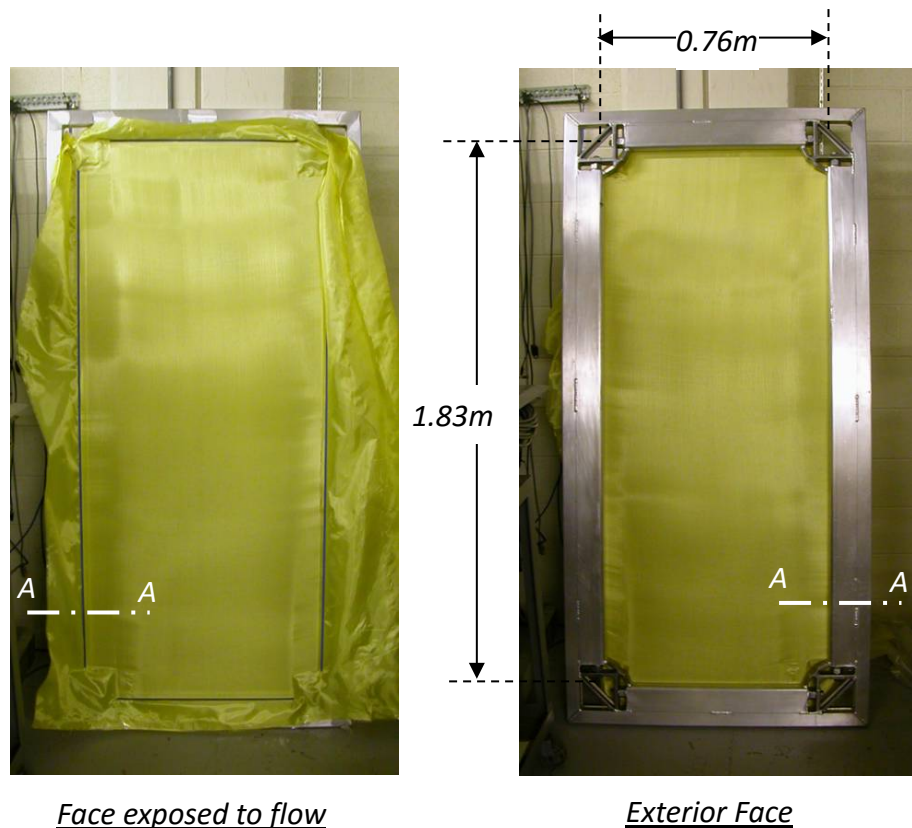

Face exposed to flow   *Exterior Face*

Figure 4.2-1. Kevlar 120 mounted in a roller-chase frame for a small-scale application, from Camargo *et al.* (2005).

seam two or more lengths of material together to obtain the desired width. This is possible, but requires care. Kevlar 120 has a plain wave which means it is unstable – a conventional sewn seam will simply pull apart under tension. To hold, the material must be folded multiple times at the seam. The seam must be then infused with glue to prevent slippage of the fibers. At the VTSWT, seams in the acoustic windows (e.g. Figure 1-2(a)), were fixed using cyanoacrylate adhesive. While this creates a comparatively thick and hard narrow band of material, 4 to 5 cm wide this did not have any detectable adverse aerodynamic or acoustic effects. Note that these seams were aligned streamwise and located as far as possible from the middle of the windows where most acoustic measurements are made.

A second option is to arrange for the fabric to be specially woven in the needed width. This has been done both at JAXA 2m wind tunnel and at the VTSWT. The costs of setting up a loom to do this are quite substantial and so this only makes sense for large quantities (≥500m) of material. However, the unused Kevlar does not degrade significantly over time (as long as it is kept out of sunlight), and windows may need to be replaced every few years, or made for special applications and so such an investment may well be worthwhile over the long term. Experience suggests that it may be difficult to find manufacturers willing or able to weave this material at widths of over 3.5m.

A simple method for mounting the Kevlar forming the acoustic windows is a 'Roller' or 'Roller Chase' frame (e.g. Figure 4.2-1 [10]). These frames are manufactured for use in the screen printing industry, and are inexpensive even in large custom sizes. Rollers within the frame are used to tension the Kevlar. The Kevlar is attached to the rollers by being trapped in a slot (Figure 4.2-2) and locked in place using nylon rods hammered into place. For small frames, such as that shown in Figure 4.2-1, the frame alone may be sufficiently strong to support the tension on the window. For larger applications, however, the needed frame size becomes impractical and it is better to attach the frame to the structure of the test section, and use it to provide the strength required.

Overall the Roller Chase frame arrangement reliably holds the Kevlar and allows it to be re-tensioned if needed. Obtaining a sufficiently uniform tension to avoid loose areas takes practice and technique partly because the frame only provides a single tension adjustment for each side of the window and partly because the strength of the Kevlar cloth prevents it from being stretched to accommodate significant imperfections in its mounting. As a practical matter this requires that it be possible to lay the frame on a horizontal surface (usually a floor) so that the Kevlar cloth can be draped uniformly over it before the nylon rods are inserted. Horizontal placement also allows for a standard gravity-based tension meter (e.g. Newman ST-Meter 2E) to be used to monitor the tension. This means that, for arrangements where the acoustic windows are mounted
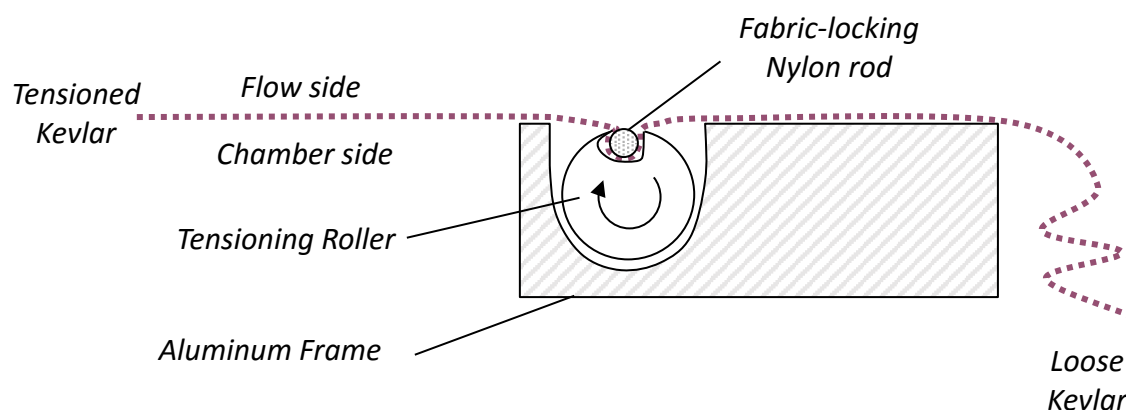
Figure 4.2-2. Schematic showing cross section through a roller chase frame, adapted from Camargo *et al.* (2005).
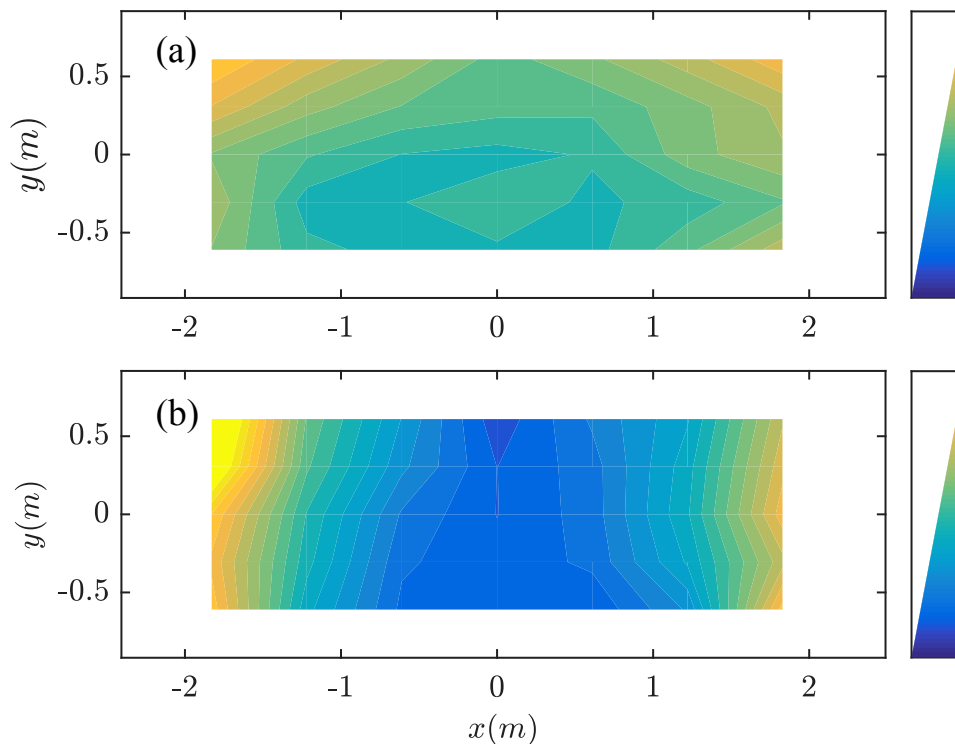
Figure 4.2-3. Pretension distribution on the port-side acoustic window of the Virginia Tech Stability Wind Tunnel anechoic test section, from Brown (2016).

vertically and the wind tunnel structure is used to provide some of the strength to support the window tension, the final tension must be estimated unless a tension meter that can function on a vertically oriented surface is available. There appear to be no commercially available devices that do this but Brown [11] describes the design of a handheld tension meter with this capability. Alternatively, if a uniform pressure difference can be imposed upon the acoustic window after mounting (such as by slightly pressurizing the anechoic chamber) then it is possible to infer the unloaded tension distribution from camera-based measurements of the strains in the window [11]. Figure 4.2-3 show measurements using a custom-built hand-held meter of the tension distribution in the port-side acoustic window if the VTSWT anechoic test section with no flow. Notice that the tension values deviate fairly substantially from the nominal 1500 N/m, particularly in the vertical component. Fortunately, tension variations have little effect on aerodynamic corrections [11] but are important if detailed finite element modeling of the acoustic windows is of interest.

Since the acoustic windows deflect under aerodynamic load, it is important that their installation be designed so that strain in the windows does not open up gaps where they meet with other test section walls. One such design, used at the VTSWT, is shown in Figure 4.2-4. The frame holding the Kevlar window is significantly wider than side-wall of the test section so that the window extends beneath the test section floor and above its ceiling. This simplifies the structural support of the frame, making it independent of the hardware supporting the floor and ceiling flow surfaces and containing the acoustic treatment behind them. It also creates clean right angles at the test section corners. Rare-earth magnets are placed on the outside of the window to maintain contact between the acoustic window and the steel strip sides of the floor and ceiling. This seems to lower some of the load on the rollers in the frame when the tunnel is in operation, reducing the chances of the Kevlar pulling off a portion of the rollers inside the frame (a rare but time-consuming occurrence). They also serve as an early warning system, as the magnets will start to drop away if the aerodynamic loads become extreme,
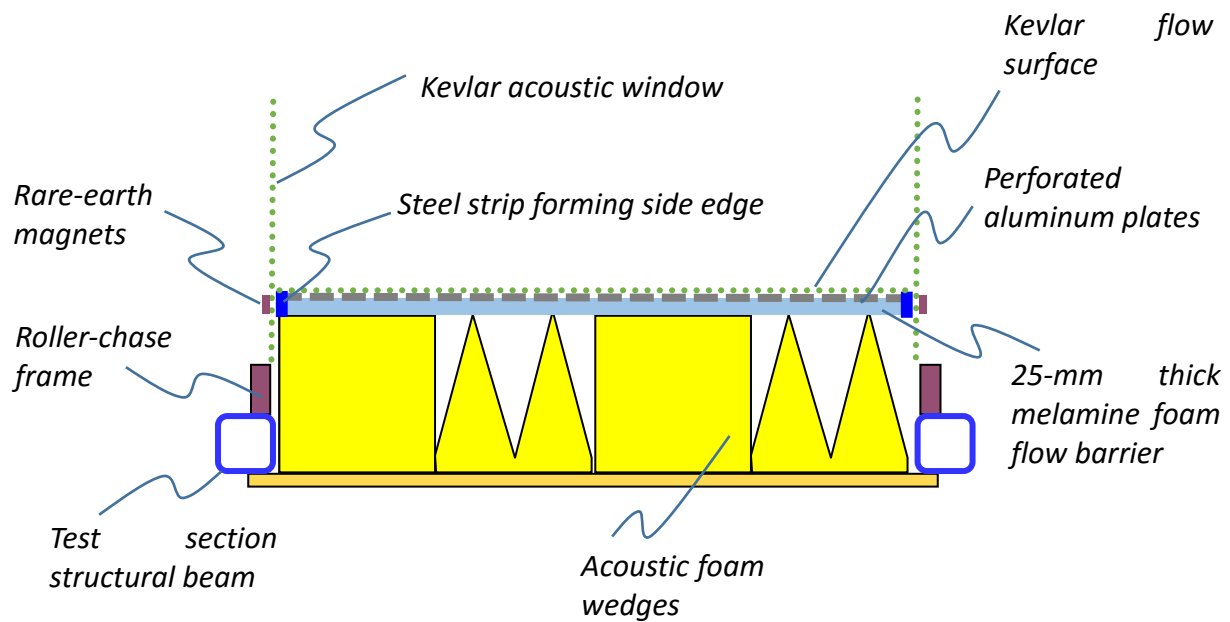
Figure 4.2-4. Cross sectional schematic through the lower wall of the VTSWT anechoic test section

Figure 4.2-5. Rare-earth magnets used to maintain contact between the acoustic windows and the side edges of the test section floor and ceiling, VTSWT.

risking window failure. Only one such event has ever occurred at the VTSWT, before magnets were introduced. A Kevlar window tore when running at top speed as a result of overloading and being stretched over the sharp edge of a spacer placed beneath it. While no lasting damage (other than to the window) was sustained, the event was sufficiently violent that safety rules were introduced prohibiting users from being in the anechoic chambers at flow speeds above 30m/s. We are also careful to avoid contact between the windows and sharp edges that might abrade them and cut through the Kevlar fibers.

4.3   Design of other test section surfaces

The acoustic windows are not the only surfaces in the test section that need special attention. Minimizing sound reflections from other surfaces can also be important in eliminating spurious reflections and reducing parasitic noise contamination of sound measurements. Acoustic absorbers are easily manufactured and come in a variety of designs (e.g. acoustic wedges, foam-filled boxes). The problem is covering these with an acoustically transparent and structurally adequate flow surface that is not itself a source of flow noise. A common arrangement is to use perforated metal plates covered on the flow side with a metal weave or fabric material. Alexander and Devenport [12, 13] and Nelson [14] have studied flow noise generated by perforated plates and coverings used with absorbers. Sound appears to be generated in two frequency regimes – high-frequency noise associated with flow over the fine weave of the covering, and low-frequency noise associated with scattering from the underlying perforate. Alexander and Devenport [12] recommend high open area ratio perforate with small-diameter holes, combined with a high thread-count cloth covering for the quietest flow surface. The VTSWT anechoic test section uses two different combinations. The test section ceiling panels are made from 4.8-mm thick perforated aluminum plate with a 51% open area ratio made with 19-mm diameter holes, covered with Kevlar 120. The floor panels also use Kevlar 120, but are made from cast aluminum floor grates (manufactured for ventilation of computer-room floors) with a 56% open area ratio. In terms of flow noise, Kevlar 120 compares with the quietest flow surfaces [13]. Though it is not the optimum it appears more durable than the fine flow-aligned wire weaves that produce the lowest sound.

Acoustically absorbent flow surfaces are not very compatible with pressure gradients generated by large models. A significant pressure difference within the flow over a porous surface will tend to drive flow through the acoustic treatment. This will result in new parasitic sources (particularly where air exits the treatment), can compromise the flow causing local separation, and in severe cases can tear the cloth covering forming the flow surface from the underlying perforate. Several precautions can prevent this from becoming a problem. First, placing an acoustic foam sheet (e.g. 25-mm thick melamine) between the back of the perforate/cloth flow surface (e.g. Figure 4.2-4) and the sound absorbing wedges or material prevents small pressure gradients from becoming a problem without significantly altering the acoustic performance. Second, breaking up the sound absorbing volume with air-tight barriers at frequent streamwise intervals prevents significant streamwise flow developing within the treatment, which can be a problem when testing high-drag models. Finally, and counter-intuitively, replacing acoustically absorbent surfaces with hard flow surfaces in the immediate vicinity of the model can be particularly beneficial. Figure 1-2(a) shows a 0.91-m chord NACA 0012 airfoil under test in the anechoic test section of the VTSWT. Hard-wall panels have been used on the test section floor and ceiling over the full width of the test section and about 1m upstream and downstream of the mid chord of the airfoil. The hard panels eliminate parasitic sources associated with the intense airfoil pressure gradients acting on an acoustically treated surface, but also act as reflectors of the sound generated by the model. However, from the perspective of a microphone system measuring the sound produced from the model (Figure 1-2(b)) these reflections produce sources that appear either below or above the test section, and thus are easily eliminated in processing.

4.4   Material properties of Kevlar

Kevlar (also known as Aramid) has become the material of choice to for the acoustic windows of hybrid anechoic tunnels, specifically Kevlar 120. This is because of the work of Jaeger *et al.* [15] who were interested in coverings for a phased array mounted in a wind tunnel wall that would reduce microphone self noise as compared to an uncovered array. Unlike fiberglass cloth and a stainless-steel screen, Kevlar cloth was able to withstand prolonged exposure to the flow. Of the three Kevlar surfaces studied Kevlar 120, combining light weight and plain weave, was found to have the lowest insertion loss, rising gradually with frequency to about 2dB at 20kHz.

Detailed documentation of the properties of Kevlar 120, with relevance to wind-tunnel applications, is provided by Brown [11]. This is a plain weave scrim made from Kevlar 49 fiber with 13.4 threads per centimeter in both the warp and weft directions. The scrim is porous and extraordinarily light, factors that both contribute to its acoustic transparency. Despite containing about 3 km of fiber, each square meter weighs only 58 g. The fibers are therefore very thin and the material has a nominal overall thickness of only 0.08 mm (a 500m roll of Kevlar 120 is less than 0.3-m in diameter). The porosity of the Kevlar appears to be dependent upon the supplier, apparently because the thickness of the fibers in the plane of the cloth depends on details of the weaving process. Brown [11] records open area ratios of 5.9% for stock material supplied by Hexcel corporation, 1.8% for custom woven cloth from EAS Fiberglass Company, and 3.9% for material obtained from a third (unspecified) manufacturer used in the JAXA 2m Low Speed Wind Tunnel, despite accurate thread counts. While all these materials were found to work well, the variations mean that measurement of the insertion loss and through-flow properties of the specific material used are necessary to ensure accurate aerodynamic and acoustic correction of measurements made in the test section.

Accounting for the bowing of the acoustic windows is part of the aerodynamic correction, and thus the mechanical properties of the Kevlar scrim must be known. As part of a low order correction model, assuming the Kevlar behaves as a thin isotropic membrane under uniform isotropic tension, Devenport *et al.* [9] used a tension modulus of 2.64×10^6 N/m. This was obtained from the known bulk modulus for Kevlar 49, of 126 GPa, assuming an equivalent membrane thickness of 0.021-mm. This was found to provide provided accurate corrections under a range of conditions. Brown [11] confirmed the accuracy of this approach, but also found that accounting for anisotropy in the material and the non-uniformity and anisotropy in the tension, gave considerably lower values of the modulus. Specifically, he found the effective moduli in the warp and weft directions to be 13.3 and 31.2 GPa respectively. The moduli are reduced from the pure material value because the Kevlar scrim can be stretched by uncrimping as well as by elastic extension of the individual fibers. Brown [11] provides further properties useful if a full finite element simulation of an acoustic window is desired, such as used when inferring the wall pressure boundary condition from the window deflection. It is known that Kevlar can degrade under UV light, compromising its mechanical properties. While this is definitely true for sunlight, degradation under normal fluorescent lighting has proved negligible at the VT Stability Tunnel, with acoustic windows giving many years of service.

Another important property of the Kevlar is its smoothness compared to alternatives. Flow over a rough surface generates noise. The roughness noise spectrum is given by the product of the wavenumber spectrum of the surface slope and the surface pressure spectrum [16], and varies in intensity as the roughness height squared. The smoothness of the Kevlar means that it produces a low sound level, but this may not be negligible when high frequency measurements are desired. The 13.4 threads per cm in Kevlar 120 would be expected to produce a roughness noise peak at about 50 kHz for a free stream velocity of 50 m/s, though this source may be visible at significantly lower frequencies if the facility is particularly quiet. Fortunately, roughness noise is radiated in streamwise and cross-stream dipoles parallel to the acoustic window, thus sound measurements made along directions perpendicular to the window will be least affected.

5.0 OPERATIONS

This section provides a description of operation of a large scale hybrid anechoic facility. The purpose is to provide a basis for the facility design and development discussion in section 4. This description is based on operational experience from work done with the anechoic test section of the Virginia Tech Stability Wind Tunnel (VTSWT).

5.1   Monitoring of reference conditions

Free stream dynamic pressure is monitored using pressures measured at static taps located in the walls of the wind tunnel settling chamber and contraction sensed using a precision transducer (Datametrics Barocel 590D with traceable calibration). Two taps are used at each location at the mid height of the two side-walls and averaged. The calibration of the settling chamber and contraction pressure taps is determined using measurements with a Pitot static probe located at the model position in the empty test section, and thus accounts for any pressure gradient effects within the test section. This calibration is regularly re-verified using static pressure taps installed in the test section floor. Temperature in the test section is monitored using an Omega Thermistor type 44004 (accuracy ±0.2°C) located at the test section entrance.

Pressures in the anechoic chamber pressures are also monitored during testing. While these are not used in reducing measurements, they can be compared with pressures calculated as part of the aerodynamic corrections and form part of the test section boundary conditions.

5.2   Aerodynamic corrections

A wide variety of aeroacoustic tests are accommodated in the VTSWT, including landing gear [17, 18, 19], fan inflow distortion [20, 21, 22, 23], UAVs, high-lift systems [24, 25] and fundamental boundary layer studies [26]. The commonest configurations tested in the anechoic test section, however, are two dimensional airfoils (e.g. Figure 1-2), usually for wind-turbine applications. The airfoils are mounted vertically and studied over a range of angles of attack. Airfoil chord lengths up to 0.91-m (chord length to test section width ratio of 0.5) are regularly tested and produce accurate aerodynamic measurements, judged by matching measurements made in the hard wall test section.

Aerodynamic corrections are made simultaneously with measurements, using the method of Devenport *et al.*[9]. A two-dimensional panel method is used to represent the side-walls of the test section, including the acoustic windows. Each wall is represented by close to 100 source panels that extend 11 test section widths h upstream and downstream of the airfoil quarter chord location (further than the physical test section walls). Panel lengths are varied to provide the maximum resolution ($3.2\%h$) closest to the airfoil. The lift, drag and solid blockage of the airfoil are represented in terms of singularities located at the model quarter chord location with strengths obtained using standard relations [27]. Once the flow over these singularities is solved, consistent with the wall boundary conditions, the strengths of the panels provide the influence of the walls on the velocities and velocity gradients at the quarter chord location. These are then used to correct the aerodynamic measurements using standard relations derived from the results of Allen and Vicente [27].

Over the Kevlar acoustic windows the boundary condition includes both transpiration through and deflection of the Kevlar window under load. Transpiration is calculated using an empirical relation between the pressure drop across the Kevlar Δp and the average flow velocity v through it, established by measurements made on the specific Kevlar window material in use using a purpose-built rig, e.g. see Brown[11]. In dimensional form this empirical relation is,

(5.1)

$$v = k_c \Delta p^{0.5} \left(\frac{\Delta p}{\Delta p + k_p} \right)^{0.073}$$

where k_c=0.0625 m/s√Pa and k_p=50 Pa for the 5.9% open aero ratio Hexcel Kevlar 120 studied by Devenport *et al.*[9]. These values are 0.0250 m/s√Pa and 1730 Pa, respectively, for 1.8% open area ratio custom woven cloth from EAS Fiberglass Company. A non-dimensional form of equation 5.1 that is less material specific is provided by Brown [11]. The calculation of the pressure difference requires that the pressure in the chambers
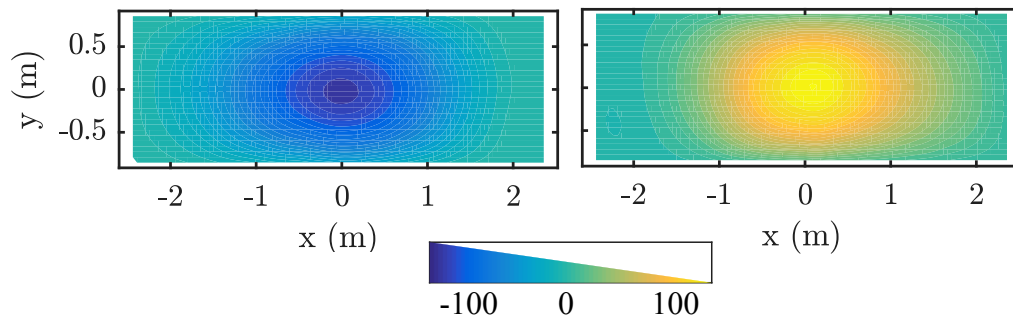
Figure 5.2-1. Kevlar window deflections in the VTSWT generated using a 0.91-m chord NACA 0012 airfoil model at 12 degrees angle of attack, generated at a free stream dynamic pressure of 3110 Pa (75 m/s), from Brown (2016). Flow is from left to right.
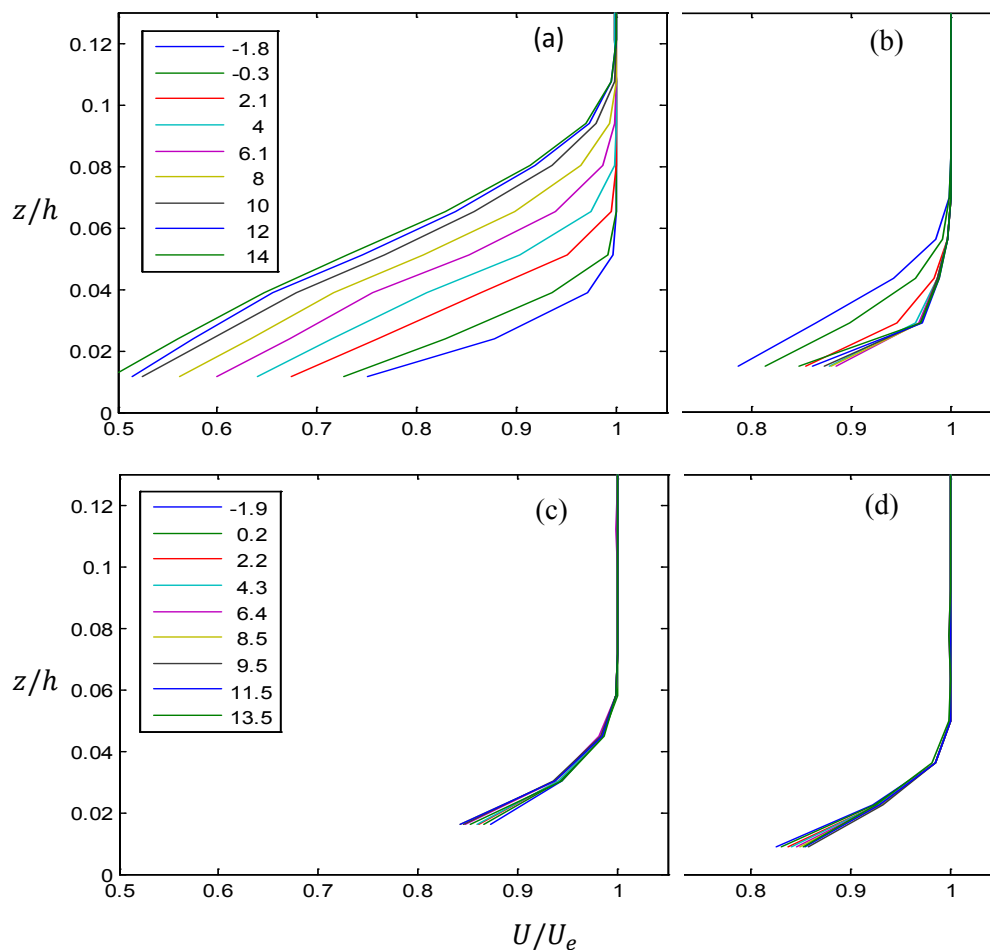

Figure 5.2-2 Boundary layer velocity profiles measured at the mid-height of the side walls in the test sections of the VTSWT with a 0.62-m chord DU96-W300 airfoil 61 m/s, normalized on test section width *h*. Legend shows airfoil angle of attack in degrees relative to zero lift. (a) Suction and (b) and pressure side walls of the hybrid test section, measurement 2.74-m downstream of airfoil quarter chord. (c) Suction and (d) pressure side walls of the hard-wall test section 1.7-m downstream of airfoil quarter chord.

also be determined, and this is computed iteratively using a mass balance that accounts both for overall conservation and for the leakage of air between the chambers. The leakage is characterized in terms an effective

area, measured by progressively pressurizing the chambers while sealing the acoustic windows. The deflection of the Kevlar windows under the pressure difference is calculated through a finite difference solution of a simplified membrane equation assuming constant isotropic tension, isotropic tension modulus and negligible shear component for the Kevlar. This calculation requires to input the unloaded tension of the windows which is re-measured when a new window is mounted or a window is tightened, and is typically taken to be 1500N/m. Kevlar deflections are spanwise averaged to give the needed panel method boundary condition. This complete iterative calculation can be completed in a few seconds on a laptop and thus is integrated with the measurement process. Corrections for three-dimensional configurations appear small and so no standard approach has yet evolved. Brown [11] describes the latest method for wings, using an extension of the two-dimensional panel method approach.

The deflection of the acoustic windows under aerodynamic load is not insignificant – at high speed for large models the load can reach a significant fraction of a ton. While deflections are usually estimated for the purposes of aerodynamic correction, rather than directly measured, such measurements have been made in several studies. Figure 5.2-1 shows that acoustic window deflections for a large airfoil model can exceed 100mm at the center of the windows.

The porosity of the acoustic windows also leads to more rapid boundary layer growth on the walls of the acoustic test section than occurs in a hard wall test section. Figure 5.2-2 shows boundary layer profiles measured on the side walls toward the rear of the anechoic and aerodynamic test sections with the same 0.61-m chord (*h/c*=0.33) airfoil installed over a range of angles of attack. The boundary layer thicknesses in the hard-wall test section never exceed 6% of the test section width. In the anechoic test section, however, the side-wall boundary layer nearest the suction side of the airfoil reaches a thickness of almost double this. This thickening is what is modeled in Equation 5.1.

5.3   Acoustic corrections

Acoustic corrections for refraction are made using the method of Amiet [28, 29] and insertion loss corrections for the transmission of sound through the Kevlar windows are made using curve fits of the type reported by Devenport *et al.* [9], see also Glegg and Devenport . Like the porosity relation the insertion loss relations are material (and manufacturer) specific. For Hexcel Kevlar 120 the Kevlar losses in dB, $\Delta_{Kevlar}(dB)$ with no flow are

$$\Delta_{Kevlar}(dB) = 0.0059F^2 + 0.0145F$$

(5.2)

and the additional flow-related losses through the test section, $\Delta_{flow}(dB)$, are

$$\Delta_{flow}(dB) = (1 - e^{-1.057F})(5.4316M + 88.95M^2)$$

(5.3)

where, in both curve fits, F is the frequency in kilohertz. These can be measured using a speaker and microphone placed in opposite anechoic chambers and used to measure the sound transmission through the entire test section, including both acoustic windows, of which the insertion losses are half [2].

These relations are plotted in Figure 5.3-1. Static losses are small and remain less than 1dB below 10kHz. Flow-related losses, representing the effect of shear, increase with frequency and Mach number reaching about 7dB at 10kHz and Mach 0.25. As long as the corrections are applied, however, the attenuation is not usually important since parasitic sources are equally attenuated as sources of interest.
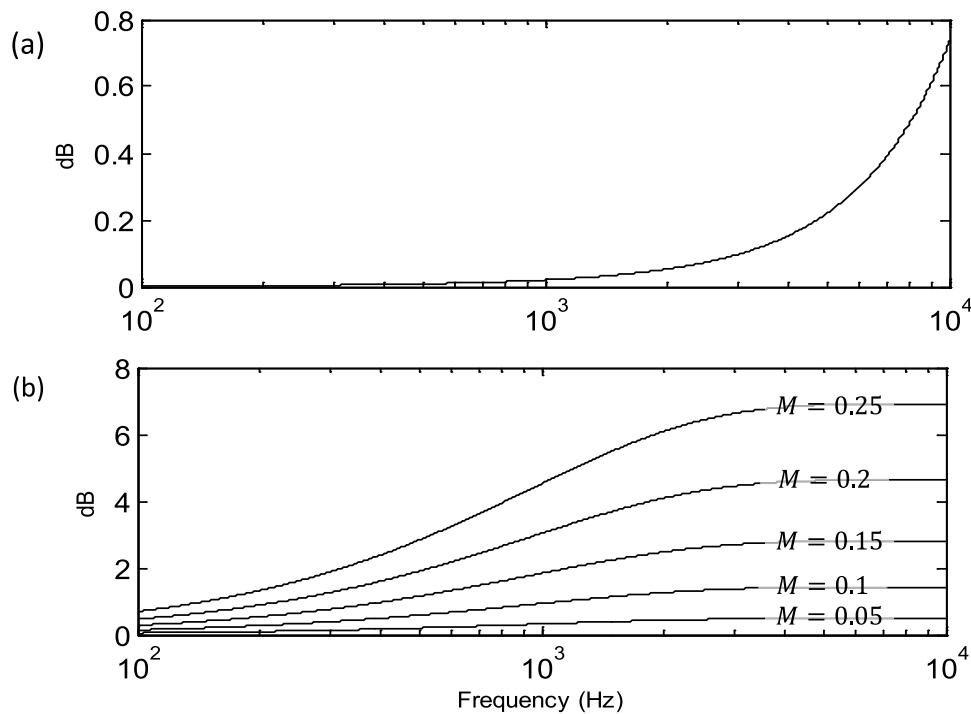
Figure 5.3-1. Insertion losses through the Kevlar acoustic window of Devenport *et al.* (2013). (a) Static losses (equation 5.2), (b) Additional flow-related losses (equation 5.3).

5.4   Instrumentation

Acoustic measurements are made in the chambers using single microphones and phased arrays. Figure 5.4-1 shows a 1.1-m diameter 117 microphone phased array sized to work as a general purpose, moveable instrument, behind the 4.2-m 1.85-m acoustic windows. The array uses Panasonic electret microphones type WM-64PNT arranged on a carbon-fiber disk in nine spiral arms.

The Kevlar-window arrangement allows for a particularly large receiving area, however, and arrays can be configured to take advantage of this. Figure 5.4-2(a) shows a 251 channel phased array designed with this in mind. The array uses G.R.A.S Type 40PH-S5 free field microphones with a frequency range of 10 Hz to 20 kHz and a dynamic range of 32 dB to 135 dB. The microphones are arranged in four interwoven spirals each made up of about 62 microphones and centered on a different streamwise position. Maximum and minimum microphone separation are 3.82 m and 30 mm, respectively. In the configuration shown in Figure 5.4-2(a) this instrument functions as 'pletharray' [30] where the sound may be analyzed using overlapping sub-arrays. This provides both source location and identification in three-dimensions and directivity measurements within a single device. In the configuration shown in Figure 5.4-2(b) the same array has been split in half with one half placed in each anechoic chamber and oriented such that the combination can be used to beamform sources in the test section cross section (in this case, over the face of a propulsion rotor disk). Such arrangements are a subject of ongoing research since they challenge standard beamforming algorithms.

Laser-based measurements are also feasible in the hybrid anechoic arrangement see, for example, the PIV studies of Murray [31], Figure 5.4-3.. The relatively small amount of air exchange between the test section and chambers greatly reduces the extent to which the acoustic treatment of the chambers are exposed to seed material. Seed material does tend to contaminate treatment in acoustic absorbers beneath the test section floor

Figure 5.4-1 117-microphone phased array system. Photo courtesy Patricio Ravetta, AVEC Inc.
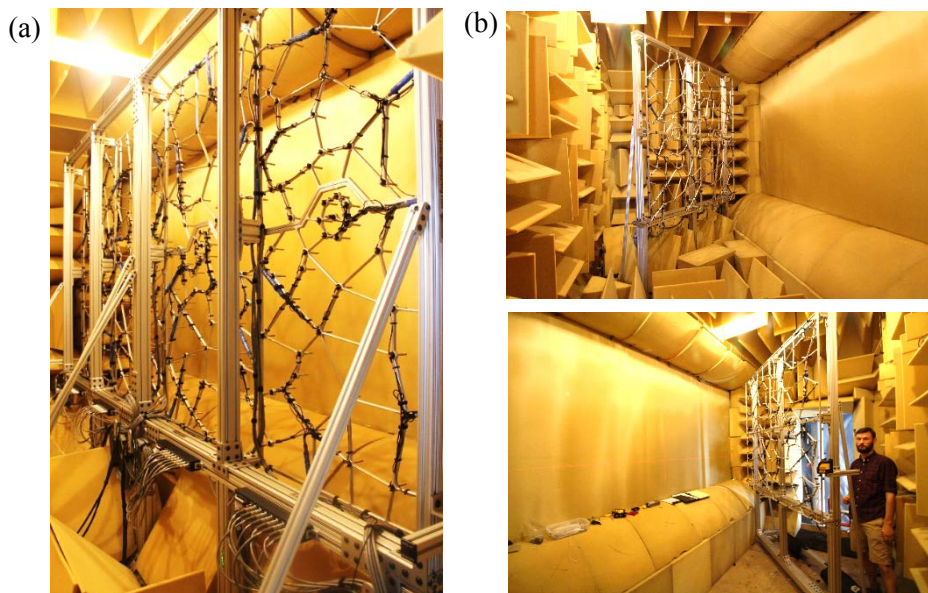
(a)

(b)

Figure 5.4-2 Configurable 251-microphone phased array (a) spanning the entire receiving area of the starboard side acoustic window of the VTSWT, and (b) split between the port and starboard side chambers for beamforming in planes cross-sectional to the flow, Part (b) images from Hickling *et al.* (2017).

towards its downstream end. However, this area has been found not to be critical to the acoustic performance of the facility and the replacement of treatment when needed in this limited area is practical. Standard seeding
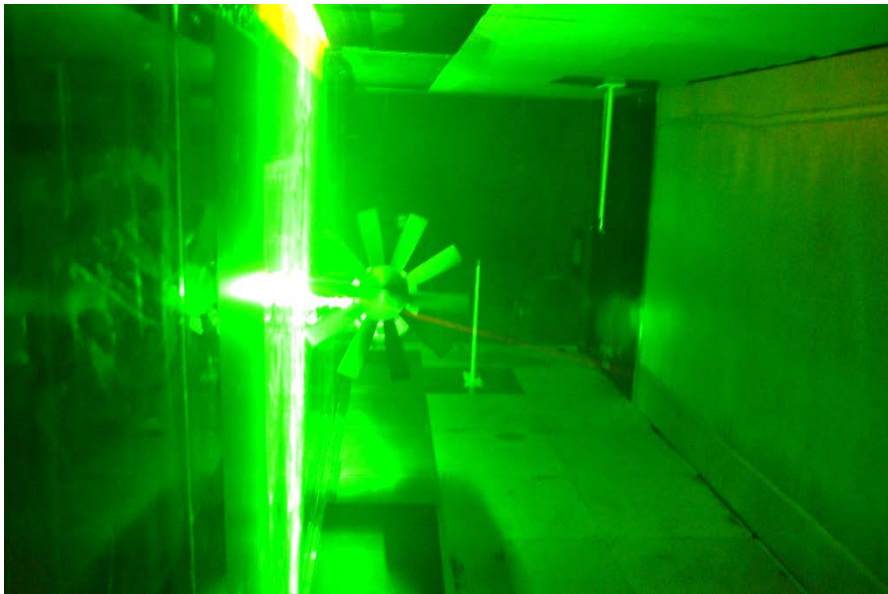
Figure 5.4-3 PIV Testing of the flow around a model rotor system in hemi-anechoic configuration as part of the study of Murray (2016).

material (Di-Ethyl-Hexyl-Sebacat oil) has not been observed to have any significant detrimental effect on the Kevlar cloth.

5.5   Application example

In this section we outline a recent example showing aerodynamic and acoustic measurements made in the VTSWT hybrid anechoic test section, their correction and their comparison with measurements made at otherwise identical conditions in the hard-wall aerodynamic section.

Measurements were made of the aerodynamic and acoustic characteristics of a DU91-W250 airfoil model. The full-span model (Figure 5.5-1) has a chord of 0.90-m as was manufactured from aluminium in the Aerospace and Ocean Engineering Machine Shop at Virginia Tech by assembling separately machined 50.8-mm thick laminates while maintaining hermetically sealed and aerodynamically smooth joints. It represents the upper end of model sizes regularly tested in this facility with chord and thickness to test section width ratios of 0.49 and 0.12 respectively. The model includes 80 half-millimeter diameter pressure taps located around midspan used to measure detailed pressure distributions that are integrated to obtain lift and moment coefficients. Acoustic measurements of trailing edge noise for this airfoil were made with both the 117 microphone phased array of Figure 5.4-1 located in the starboard side anechoic chamber, and directed at the pressure side of the airfoil, and the 251-microphone array of Figure 5.4-2(a) located in the port side chamber and directed at the airfoil suction side. Measurements were made with the airfoil in clean condition (untripped, natural transition verified through naphthalene flow visualization) for a chord Reynolds number of 3.0 million and Mach number of 0.17.

Figure 5.5-1 DU91-W250 airfoil model mounted in the VTSWT hybrid anechoic test section.

Figure 5.5-2 compares lift coefficient plotted vs. angle of attack for the measurement in the anechoic test section and for matching conditions in the hard-wall test section. The agreement, once aerodynamic corrections have been applied, is quite good including in the positive stall region. It is important to be aware that the corrections are *a priori* and involve no adjustable constants. All physical constants required for the anechoic corrections, such as those of the porosity relation (equation 5.1) are determined independently.

It is interesting to compare the uncorrected data in Figure 5.5-2. For positive angles of attack less than about 9 degrees the absolute corrections to the lift curve are actually less for the hybrid anechoic test section than they are for the hard-wall. This is because the transpiration of air through the porous Kevlar acts to reduce the angle of attack counter-acting some of the blockage effect. For angles of attack above 10 degrees, corrections for the hybrid test section exceed those of the hard-wall test section. This is because the bowing of the Kevlar windows under the high aerodynamic load at these conditions effectively narrows the test section, increasing blockage above the hard wall value by more than is compensated for by the porosity.

The correction method is illustrated in Figures 5.5-3 and 5.5-4. Here we show results from a test section panel method calculation very like those used to determine the corrections for the hybrid anechoic test section data. Note that the calculations depicted fully resolve the airfoil, whereas the airfoil is modeled only using a combined source, doublet, vortex singularity at the quarter chord when the correction is estimated. This makes no significant difference to the results, but seeing the whole airfoil makes streamline patterns intuitively easier to interpret.
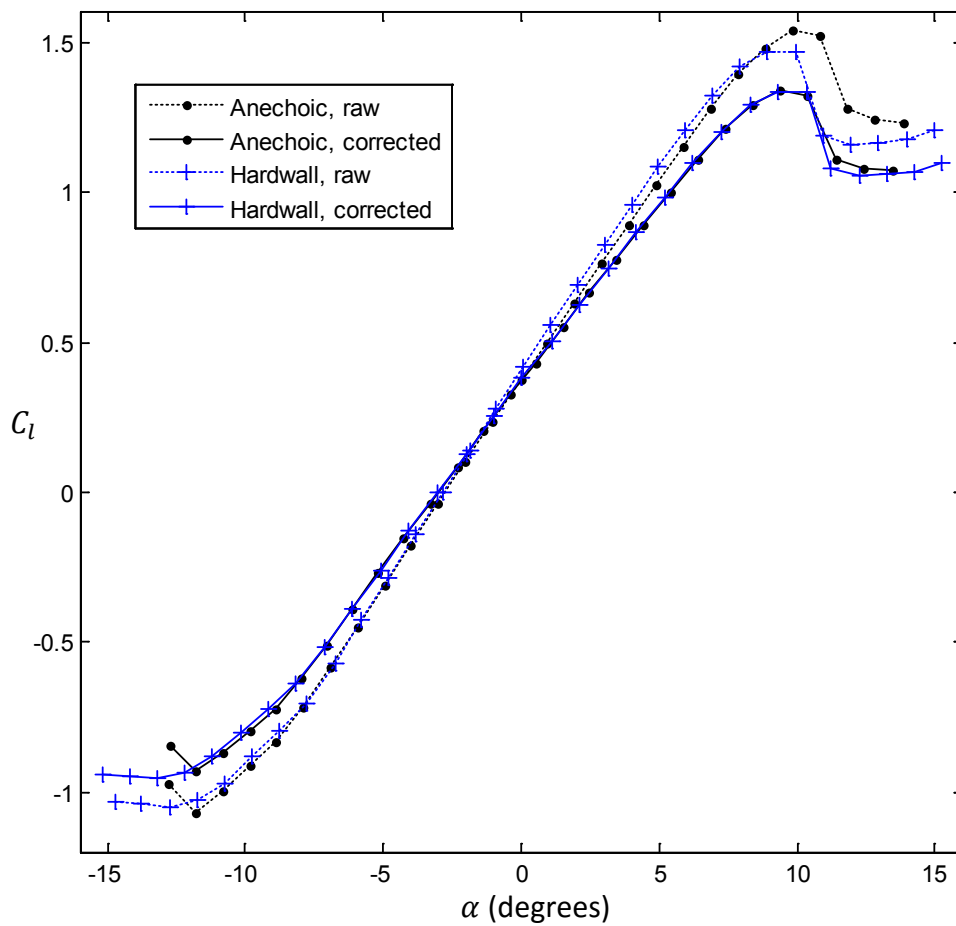
Figure 5.5-2 Lift coefficient as a function of angle of attack for the clean DU91-W250 airfoil model at 3.0 million chord Reynolds number measured in hybrid anechoic and hard wall test sections.
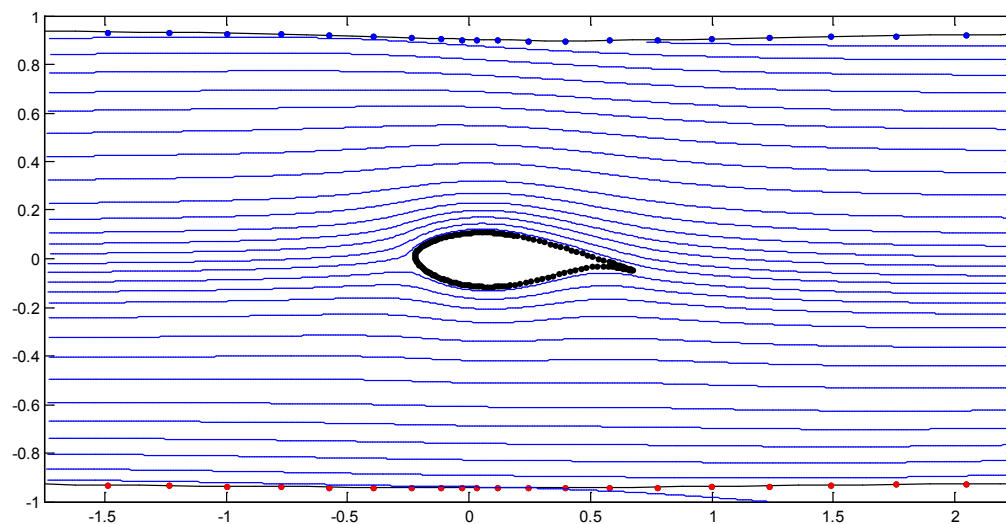

Figure 5.5-3 Test-section panel method simulation for the DU91-W250 at 4 degrees angle of attack (geometric). Distances in meters.

Streamline patterns are shown in Figure 5.5-3. Included here (to scale) is the deformation of the acoustic windows forming the test section walls. Note that the blue and red dots represent the control points of the source panels used to model the walls, and it is the spanwise-averaged deformation that is represented. The acoustic window nearest to the suction side of the airfoil is drawn inward whereas that nearest the pressure side bows outward under the pressure field. The complete deformation of the windows is shown in Figure 5.5-4 and the pressure differences acting on them in Figure 5.5-5. It is the deformation that acts to increase blockage compared to the hard-wall test section. Figure 5.5-3 also shows streamlines on the suction side wall entering the test section (on the top right of the figure), and leaving the test section through the pressure side wall (bottom right), as a result of transpiration through the Kevlar. It is this motion that cancels some of the angle of attack increase due to blockage.
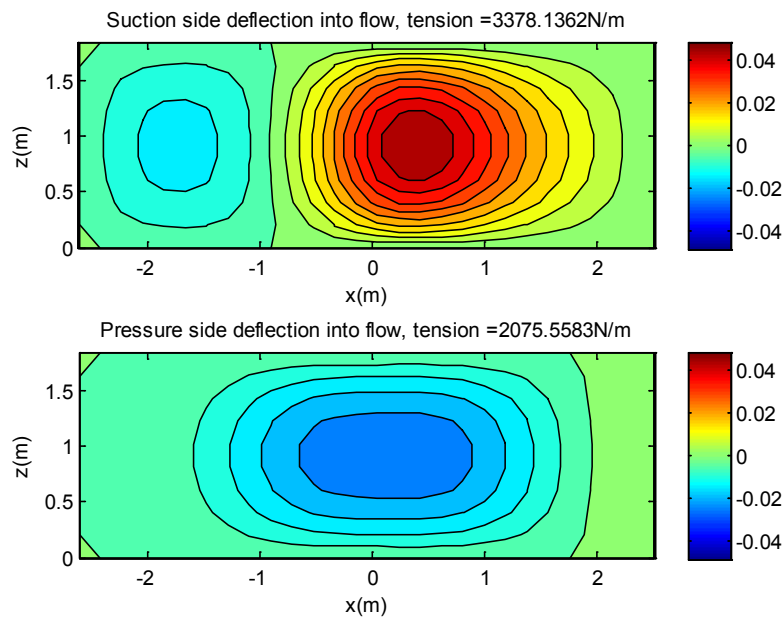
Figure 5.5-4 Computed acoustic window deflections for the DU91-W250 at 4 degrees angle of attack (geometric). Distances in meters.
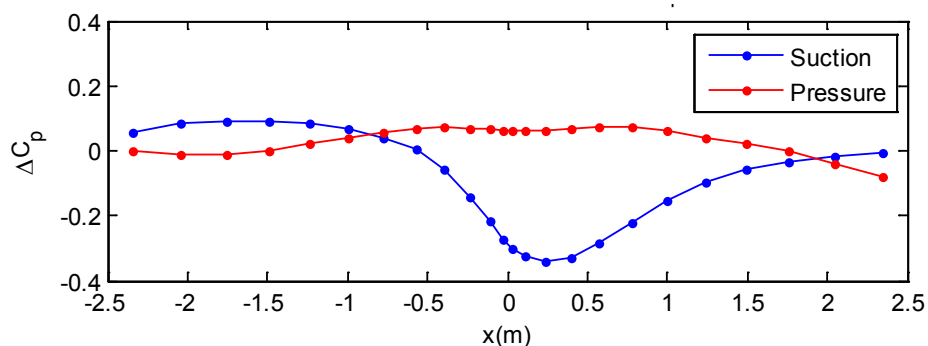

Figure 5.5-5 Computed pressure differences across the acoustic windows for the DU91-W250 at 4 degrees angle of attack (geometric). Distances in meters.

Figures 5.5-6(a) and (b) show sample beam-form results from the 117-microphone phased array for a 12th octave band around 1700Hz. The trailing edge noise is clearly visible in the vertical stripe at the airfoil trailing edge. Also clearly is the improved resolution of the 251-microphone phased array in the streamwise direction. This derives from its wide aperture (3.66-m in x) and the fact that the Kevlar window allows it to be placed only 0.75-m from the flow along that entire length. These same characteristics enable this array to be used for source identification to much lower frequencies. Figure 5.5-7 shows the same measurement at 355Hz where the trailing edge source is still being resolved by this instrument. Note that the weak apparent source appearing
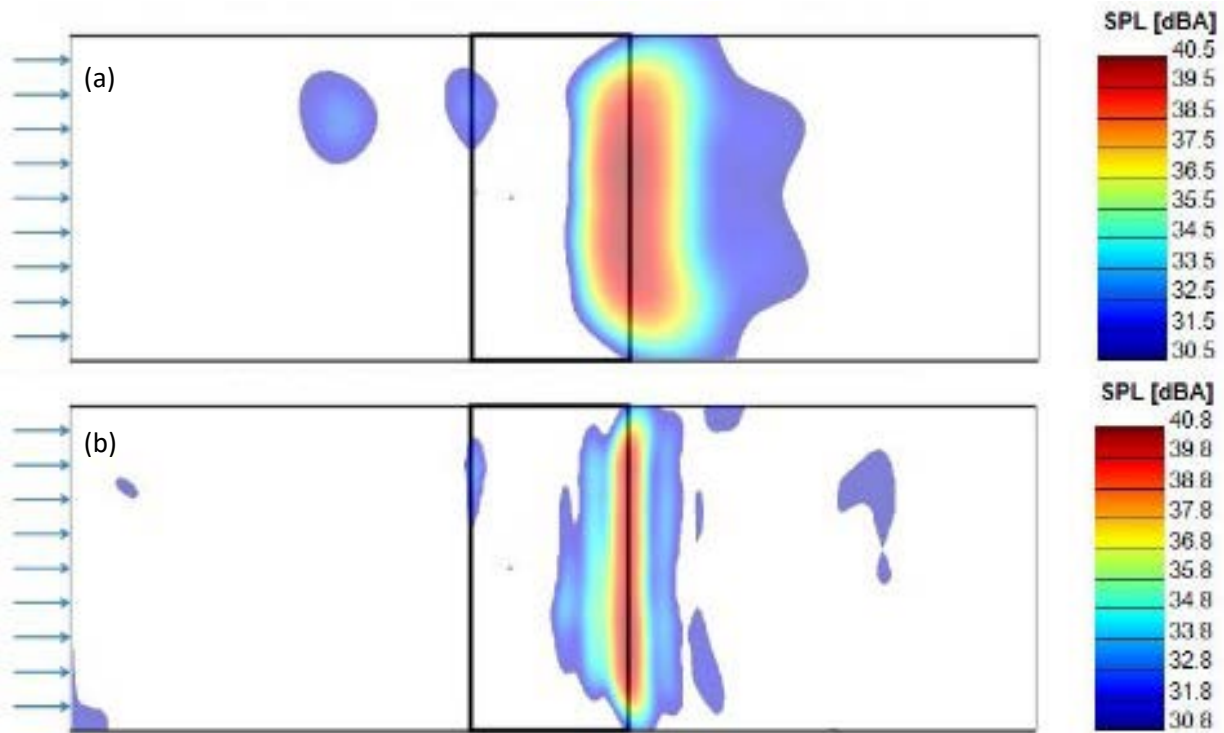
Figure 5.5-6. Beamform maps at 1.7 kHz of trailing edge noise from the clean DU91-W250 at zero angle of attack for a chord Reynolds number of 3,000,000. Maps are to scale with the airfoil indicated by the black rectangle. Data from (a) the 117-microphone spiral array, and (b) the 251-microphone rectangular array.
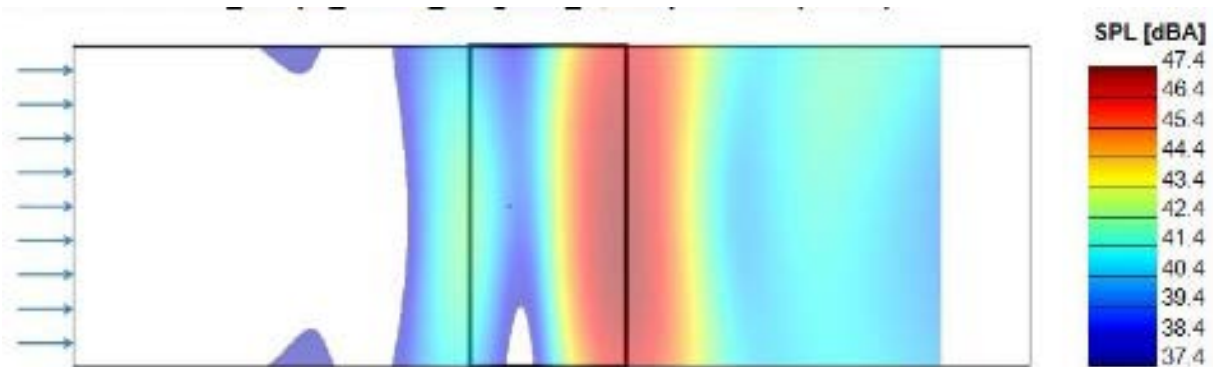

Figure 5.5-7. Beamform map at 355Hz of trailing edge noise from the clean DU91-W250 at zero angle of attack for a chord Reynolds number of 3,000,000. Map is to scale with the airfoil indicated by the black rectangle. Data from the 251-microphone rectangular array.

at the leading edge at this frequency is believed to be facility noise from upstream scattering from the leading edge.

5.0 CONCLUSIONS

The concept of the hybrid anechoic wind tunnel was introduced in these lecture notes. Two wind tunnels, the Virginia Tech Stability Wind Tunnel and the Poul la Cour Tunnel, currently under construction, were described in detail. These represent, respectively, hybrid anechoic facilities developed by retrofitting an existing aerodynamic wind tunnel, and designed from scratch. The design of the tunnels are described in detail, but the requirement for the airline design does in principle not deviate from other aeroacoustic wind tunnels. However, the design of the test section is different from other acoustic facilities and these designs are described as well. Design considerations for the test section for both new and retrofitted facilities are described, from overall test section configuration to material properties of Kevlar cloth used to form acoustic windows. Operational details of this type of wind tunnel are explained. Whereas the Poul la Cour Tunnel is in construction and experience with measurements has not yet been build up, experience with the hybrid anechoic wind tunnel concept has been build up in the Virginia Tech Stability Tunnel over a decade. Here it has shown promising results especially for tests when simultaneous measurement of lift characteristics and acoustic characteristics are needed.

ACKNOWLEDGEMENTS

REFERENCES

[1] Brooks, T.F., Pope, D.S., and Marcolini, M.A., *Airfoil Self Noise and Prediction*, vol. NASA RP 1218, NASA, 1989.

[2] Glegg, S., and Devenport, W., *Aeroacoustics of Low Mach Number Flows: Fundamentals, Analysis, and Measurement*, London: Academic Press, 2017.

[3] Moreau, S., Henner, M., G., I., Wang, M., and Roger, M., "Analysis of flow conditions in free jet experiments for studying airfoil self-noise," AIAA Journal, 2003, vol. 41, pp. 1895–1905.

[4] Ciobaca, V., Melber-Wikending, S., Wichmann, G., Bergmann, A., and Kupper, A., "Experimental and numerical studies of the low speed wind tunnel DNW-NWB's open test section towards an aeroacoustic facility," in 18th AIAA/CEAS Aeroacoustics Conference (33rd AIAA Aeroacoustics Conference), Colorado Springs, CO, 2012.

[5] Smith, B., Camargo, H., Burdisso, R., and Devenport, W.J., "Development and Testing of a Novel Acoustic Wind Tunnel Concept," in 11th AIAA/CEAS Aeroacoustics Conference, Monterey, California, 2005.

[6] Remillieux, M.C., Crede, E.D., Camargo, H.E., Burdisso, R.A., and Devenport, W.J., "Calibration and Demonstration of the New Virginia Tech Anechoic Wind Tunnel," in 14th AIAA/CEAS Aeroacoustics Conference, Vancouver, British Columbia, 2008.

[7] Choi, K., and Simpson, R., *Some Mean Velocity, Turbulence, and Unsteadiness Characteristics of the VPI&SU Stability Wind Tunnel*, Virginia Tech, Department of Aerospace and Ocean Engineering, 1987.

[8] Brown, K.A., Devenport, W., Borgoltz, A., Ura, H., and Yamamoto, K., "Towards Interference Corrections for Three-Dimensional Models in Kevlar-Walled Anechoic Test Sections," in AIAA 52nd Aerospace Sciences Meeting, National Harbor, Maryland, 2014.

[9] Devenport, W.J., Burdisso, R.A., Borgoltz, A., Ravetta, P.A., Barone, M.F., Brown, K.A., and Morton, M.A., "The Kevlar-walled anechoic wind tunnel," Journal of Sound and Vibration, 2013, vol. 332, no. 17, pp. 3971-3991.

[10] Camargo, H.E., Smith, B.S., Devenport, W.J., and Burdisso, R.A., *Evaluation and Calibration of a Prototype Acoustic Test Section for the Virginia Tech Stability Wind Tunnel*, Virginia Tech, 2005.

[11] Brown, K.A., "Understanding and Exploiting Wind Tunnels with Porous Flexible Walls for Aerodynamic Measurement," PhD dissertation, Aerospace and Ocean Engineering, Virginia Tech, 2016.

[12] Alexander, N., and Devenport, W., "Noise Produced by Fabric and Wire Mesh Covered Panels in Low-Speed Anechoic Wind Tunnels," in Aviation 2015, Dallas, TX, 2015.

[13] Alexander, W.N., and Devenport, W.J., "Noise from Boundary Layer Flow over Fabric Covered Perforate Panels," in 20th AIAA/CEAS Aeroacoustics Conference, Atlanta, GA, 2014.

[14] Nelson, P.A., "Noise Generated by Flow over Perforate Surfaces," Journal of Sound and Vibration, 1982, vol. 83, no. 1, pp. 11-26.

[15] Jaeger, S.M., Horne, W.C., and Allen, C.S., "Effect of Surface Treatment on Array Microphone Self-Noise," in 6th AIAA/CEAS Aeroacoustics Conference, Lahaina, HI, 2000.

[16] Glegg, S., and Devenport, W., "The far-field sound from rough-wall boundary layers," Proceedings of the Royal Society A: Mathematical, Physical and Engineering Sciences, 2009, vol. 465, no. 2106, pp. 1717-1734.

[17] Remillieux, M.C., Camargo, H.E., Ravetta, P.A., Burdisso, R.A., and Ng, W.F., "Novel Kevlar-Walled Wind Tunnel for Aeroacoustic Testing of a Landing Gear," AIAA Journal, 2008, vol. 46, no. 7, pp. 1631-1639.

[18] Remillieux, M.C., Camargo, H.E., Ravetta, P., Burdisso, R., and Ng, W.F., "Noise Reduction of a Model-Scale Landing Gear Measured in the Virginia Tech Aeroacoustic Wind Tunnel," in 14th AIAA/CEAS Aeroacoustics Conference, Vancouver, BC, Canada, 2008.

[19] Ravetta, P., Khorrami, M.R., Burdisso, R., and Wisda, D., "Acoustic Measurements of a Large Civil Transport Main Landing Gear Model," in 22nd AIAA/CEAS Aeroacoustics Conference, Lyon, France, 2016.

[20] Alexander, W.N., Devenport, W., Morton, M., and Glegg, S., "Noise from a Rotor Ingesting a Planar Turbulent Boundary Layer," in 19th AIAA/CEAS Aeroacoustics Conference, Berlin, 2013.

[21] Alexander, W.N., Devenport, W.J., Wisda, D., Morton, M.A., and Glegg, S.A., "Sound Radiated from a Rotor and Its Relation to Rotating Frame Measurements of Ingested Turbulence," in 20th AIAA/CEAS Aeroacoustics Conference, Atlanta, GA, 2014.

[22] Alexander, W.N., Molinaro, N.J., Hickling, C., Murray, H., Devenport, W.J., and Glegg, S.A., "Phased Array Measurements of a Rotor Ingesting a Turbulent Shear Flow," in 22nd AIAA/CEAS Aeroacoustics Conference, Lyon, France, 2016.

[23] Molinaro, N.J., Balantrapu, A.N., Hickling, C., Alexander, N., Devenport, W., and Glegg, S., "The Ingestion of Wake Turbulence into an Open Rotor," in 23rd AIAA/CEAS Aeroacoustics Conference, Denver, CO, 2017.

[24] Yamamoto, K., Ura, H., Yokokawa, Y., Nakakita, K., Camargo, H.E., Remillieux, M.C., Boor, Z., Burdisso, R., Ng, W.F., Uchida, H., Imamura, T., and Ito, T., "Aeroacoustic Testing of a High-Lift Device in the Virginia Tech Anechoic Wind Tunnel," 2009.

[25] Ito, T., Ura, K., Nakakita, K., Yokokawa, Y., Ng, W.F., Burdisso, R., Iwasaki, A., Fujita, T., Ando, N., Shimada, N., and Yamamoto, K., "Aerodynamic/Aeroacoustic testing in Anechoic Closed Test Sections of Low-speed Wind Tunnels," in 16th AIAA/CEAS Aeroacoustics Conference, Stockholm, Sweden, 2010.

[26] Meyers, T., Forest, J.B., and Devenport, W.J., "The wall-pressure spectrum of high-Reynolds-number turbulent boundary-layer flows over rough surfaces," Journal of Fluid Mechanics, 2015, vol. 768, pp. 261-293.

[27] Allen, H.J., and Vincente, W.G., *Wall Interference in a Two-Dimensional-Flow Wind Tunnel, With Consideration of the Effect of Compressibility*, NACA, 1947.

[28] Amiet, R., "Correction of open jet wind tunnel measurements for shear layer refraction," in AIAA 2nd Aero-Acoustics Conference, Hampton, VA, 1975.

[29] Amiet, R.K., "Refraction of Sound by a Shear Layer," Journal of Sound and Vibration, 1978, vol. 58, no. 4, pp. 467-482.

[30] Underbrink, J.R., "Pletharrays for Aeroacoustic Phased Array Applications," in AIAA Aviation 2015, Dallas, TX, 2015.

[31] Murray, H.H., "Turbulence and Sound Generated by a Rotor Operating Near a Wall," MS Thesis, Aerospace and Ocean Engineering, Virginia Tech, 2016.

[32] Performance of conical diffusers in incompressible flow. Technical Report ESDU-73024, Engineering Sciences Data Unit, 251-259 Regent Street, London, W1R 7AD, October 1973

[33] Performance in incompressible ow of plane-walled di_users with single-plane expansion. Technical Report ESDU-74015, Engineering Sciences Data Unit, 251-259 Regent Street, London, W1R 7AD, June 1974.

[34] B. Lindgren, J. M. Österlund, and A. V. Johansson. Measurement and calibration of guide-vane performance in expanding bends for wind-tunnels. Experiments in Fluids, 24:265-272, 1998.

[35] A. Sahlin and A. V. Johansson. Design of guide vanes for minimizing the pressure loss in sharp bends. Phys. Fluids A, 3:1934-1940, 1991.

[36] A. V. Johansson. A low speed wind-tunnel with extreme ow quality-design and tests. Proc. the 18th ICAS Congress, pages 1603-1611, 1992.

[37] M. Drela and M. B. Giles. Viscous-inviscid analysis of transonic and low Reynolds number airfoils. AIAA, 25(10):1347, 1987.

[38] T. Maeda and Y. Kondo. RTRI's Large-scale low-noise wind tunnel and wind tunnel tests. Quarterly Report of RTRI, 42(2):65-70, 2001.

[39] A. Bergmann. The Aeroacoustic Wind Tunnel DNW-NWB. In 18th AIAA/CEAS Aeroacoustics Conference (33rd AIAA Aeroacoustics Conference, 4 - 6 June 2012, Colorado Springs, CO), 2012.

[40] J. Groth and A. V. Johansson. Turbulence reduction by screens. J. Fluid Mech, 197:139-155, 1988.

[41] J. H. Downie, R. Jordinson, and F. H. Barnes. On the design of three-dimensional wind tunnel contractions. J. Royal Aeronautical Society, pages 287-295, 1984.

[42] A. V. Johansson. A low speed wind-tunnel with extreme ow quality-design and tests. Proc. the 18:th ICAS Congress, pages 1603-1611, 1992.

[43] B. Lindgren and A. V. Johansson. Evaluation of the ow quality in the low-speed MTL wind-tunnel. TRITA-MEK 2002:13, Department of Mechanics, KTH, 2002.